Catena 172 (2019) 295–312

Contents lists available at ScienceDirect

Catena

journal homepage: www.elsevier.com/locate/catena

Spatio-temporal changes of the climatic water balance in Romania as a response to precipitation and reference evapotranspiration trends during 1961–2013

Remus Prăvălie[a,b], Adrian Piticar[c], Bogdan Roșca[d], Lucian Sfîcă[e], Georgeta Bandoc[a,*], Adrian Tiscovschi[a], Cristian Patriche[d]

[a] University of Bucharest, Faculty of Geography, 1 Nicolae Bălcescu Street, 010041 Bucharest, Romania
[b] ICUB, University of Bucharest, 36–46 M. Kogălniceanu Blvd., 050107 Bucharest, Romania
[c] Babeș-Bolyai University, Faculty of Geography, 5–7 Clinicilor Street, 400006 Cluj-Napoca, Romania
[d] Romanian Academy, Iaşi Divison, Geography Department, 8 Carol I Street, 700505 Iaşi, Romania
[e] Alexandru Ioan Cuza University, Faculty of Geography and Geology, Department of Geography, 20A Carol I Street, 700506 Iaşi, Romania

ARTICLE INFO

Keywords:
Climatic water balance
Precipitation
Reference evapotranspiration
Spatio-temporal changes
Water deficit
Drier conditions
Romania

ABSTRACT

Changes in precipitation (P), evapotranspiration (ET) and, implicitly, in the climatic water balance (CWB), are imminent effects of climate warming. However, changes in the CWB, as a response to changes in P and ET, have not yet been analysed thoroughly enough in many parts of the world, including Romania. The present study explores the spatio-temporal changes of the CWB (difference between P and reference evapotranspiration, ET_o) in Romania, based on a wide range of climatic data (P, as well as temperature, relative air humidity, sunshine duration and wind speed, necessary for computing ET_o with the FAO-56 Penman-Monteith method) recorded at 70 weather stations across the country in the 1961–2013 period. As a secondary objective, the study attempts to identify the possible connections between the index's trends and large-scale atmospheric circulation, assessed based on the dynamics of certain European-scale relevant teleconnection indices. Thus, the Mann–Kendall test and *Sen's slope* methods were used to analyse CWB trends (but also P and ET_o trends, in order to explain CWB pattern changes) annually, seasonally and in the maize and wheat growing seasons. Also, the Spearman correlation procedure and a composite analysis between interannual series of teleconnection indices and CWB were used to assess the influence of atmospheric circulation on the index's variability for all analysed time scales. The results generally showed CWB decreases (for the most part of up to −2 mm/yr, yet with a relatively low statistical significance) and highlighted an overall amplification of drier conditions on all time scales, except for autumn (CWB increases, generally of up to 1 mm/yr, but with low statistical significance). Moreover, net changes of even under −200 mm/53 yrs annually and −175 mm/53 yrs in summer and for the maize and wheat growing seasons were found in the CWB. Spatially, it was found that the country's southwestern and southeastern regions are the main epicentres of drier trends, while the northwest appears to have become wetter. Overall, the negative CWB trends are due to partial P decreases (statistically insignificant) and general ET_o increases (highly statistically significant, even 100% in summer). It seems that the amplification of the climatic water deficit across the country is especially linked to the positive phases of the Arctic Oscillation and North Atlantic Oscillation, but also, in part, to those of several other teleconnection indices that affect Europe. Our results signal the necessity to adapt anthropic and ecological systems to future dryness trends countrywide, which will most likely intensify against the background of climate change expected to occur by the end of the century.

1. Introduction

We are living in the climate change era, which is one of the greatest environmental challenges of our time. While the increase in mean global temperatures has reached ~0.9 °C since the beginning of the 20th century (IPCC, 2013), global warming, the most important type of climate change, is particularly alarming when considering temporal and spatial differences of temperature pattern changes. For instance, the

* Corresponding author.
E-mail address: geobandoc@yahoo.com (G. Bandoc).

https://doi.org/10.1016/j.catena.2018.08.028
Received 7 April 2018; Received in revised form 20 July 2018; Accepted 27 August 2018
Available online 07 September 2018
0341-8162/ © 2018 Elsevier B.V. All rights reserved.

increase rate of mean global temperatures doubled after 1979 over land compared to ocean areas (Diffenbaugh and Field, 2013), anthropic systems and terrestrial ecosystems therefore becoming all the more vulnerable to this environmental perturbation. However, the most important threat of increasing temperatures in this century consists of the interaction between the atmosphere and other Earth systems possibly triggering positive feedbacks. Instances of numerous global warming autoacceleration mechanisms (e.g. snow cover decline in the arctic region that will trigger additional warming by drastically reducing albedo, or boreal forests dieback/permafrost thawing that will release large amounts of carbon/methane into the atmosphere, thus amplifying the greenhouse effect) have been well documented (Lenton et al., 2008). Theoretically, these positive feedbacks could generate an increase in mean temperatures of up to 6 °C for doubled CO_2 in the atmosphere (Hansen et al., 2008). This hypothetical scenario can however become highly unlikely if governments worldwide manage to rapidly curb down CO_2 emissions, according to the Paris Agreement that aims to stabilize warming under the 2 °C threshold throughout this century, relative to preindustrial levels (Fawcett et al., 2015).

Global warming itself is a major driving force of many environmental changes, including precipitation (P) and evapotranspiration (ET). In a warmer world, the entire Earth's water cycle changes as a result of the overall increase in rainfall, surface evaporation and plant transpiration (or evapotranspiration). However, there currently are numerous differences between such changes occurring in various global regions – certain global land areas are experiencing an increase in atmospheric humidity, while others are becoming increasingly dry (IPCC, 2013). While the additional energy that warming adds to the climate system is already activating in many regions of the globe (e.g. in the tropics) a higher amount of water in the atmosphere that influences precipitation amounts (IPCC, 2007), the net changes of the atmospheric water cycle also depend on ET dynamics. Although a warmer atmosphere will cause ET to increase especially in terrestrial areas with significant water content, the state of affairs can become significantly more complicated in a possible future scenario with higher amounts of atmospheric carbon, where plants will be likely to transpire less due to the decrease in stomatal conductance (against the background of atmospheric CO_2 excess) and, implicitly, to the decrease in the gas exchange between the biosphere and atmosphere (Bonan, 2008).

Over the past decades, significant changes in P and ET (or in climatic water balance – CWB, computed based on P and ET values) have occurred across the globe. After 1951, an apparent overall increase in annual P amounts was noted in the mid- and higher-latitudes of Northern (e.g. in the United States or in central-northern region of Europe) and Southern (Argentina and northern Australia) Hemispheres (IPCC, 2013). However, in the same period and at the same time, decreases in P amounts were recorded in Mediterranean Europe, the Sahel region, southern and eastern Africa, eastern and, in part, southeastern Asia and southeastern Australia. It can therefore be concluded that these regions experienced an increasingly intense overall humidity deficit, but, in order to obtain an accurate assessment of the climatic water deficit, ET trends must be taken into account as well, which have generally been recorded over a more recent period of time (after 1980) globally (Jung et al., 2010; Wang et al., 2010). However, based on the results of a relatively recent study that analysed global ET trends starting with the second half of the 20th century (Sheffield et al., 2012), it can be concluded that these lower P global areas have indeed experienced an intense water deficit, considering the overall increase in ET in most of the aforementioned regions.

In many instances, it is however difficult to conduct a general analysis of the CWB dynamics, in part due to the fact that ET trends are not necessarily positive in a warmer world, given the interferences of other causes (lower wind speed or decreased solar radiation in areas with higher aerosol concentrations) that appear to be responsible for the lower values this parameter has had in recent decades in many countries worldwide. Relevant examples that can illustrate this include the United States, China, India, Thailand or Australia (IPCC, 2007; Roderick et al., 2007; Fu et al., 2009). Moreover, it appears that, after 1998, soil moisture decreases in Southern Hemisphere were a major determining factor in slowing the increase of global ET (Jung et al., 2010), which highlighted other variables that can influence the ET regime on a large scale.

Advanced climate models suggest a significant possible future increase in global ET, which, despite a similar trend expected for precipitation, will strongly amplify the climatic water deficit in extensive global areas (Feng and Fu, 2013). Given these conditions, an expansion of arid environments is likely to occur especially in northwestern and southwestern North America, eastern Latin America, southern and central Europe, the Sahel region and southern Africa, eastern and northeastern Asia, and eastern Australia (Feng and Fu, 2013; Huang et al., 2016). Overall, it has been suggested that, by 2100, drylands (delimited based on the P/ET ratio) will cover as much as 56% of the global land area under the pessimistic scenario RCP8.5 (or 50% considering RCP4.5) (Huang et al., 2016), as opposed to their current share of 45%, according to the latest estimations (Prăvălie, 2016). Therefore, considering the far more aggressive expansion of land systems that will become drier compared to those expected to become wetter, it was suggested the unanimously acknowledged statement “dry gets drier, wet gets wetter” should be rephrased to “dry gets drier, but more than wet gets wetter” (Prăvălie, 2016).

The Mediterranean European region is therefore a past global hotspot of CWB change towards a humidity deficit, as certain studies directly or indirectly signalled the increasing aridity in various countries such as Spain (Vicente-Serrano et al., 2014), Italy (Colantoni et al., 2015) and Greece (Nastos et al., 2013). It is at the same time a projected epicentre of these drier trends, which also reaches the southeastern region of the continent, where Romania is located (Gao and Giorgi, 2008; Cheval et al., 2017). One of the major economic and ecological implications of these restrictive and persistent climatic conditions relate to the extensive land degradation in numerous countries in southern and southeastern Europe, including Romania (Prăvălie et al., 2017a).

Over the past ~50 years, Romania has experienced various forms of climate change (Busuioc et al., 2010; Ionita et al., 2013; Cheval et al., 2014; Marin et al., 2014; Spinoni et al., 2014; Dumitrescu et al., 2015; Croitoru et al., 2016a; Prăvălie et al., 2016a), including changes in key P (Marin et al., 2014; Dumitrescu et al., 2015; Croitoru et al., 2016b) and ET (Croitoru et al., 2013a) parameters. While national annual precipitation amounts generally remained stable (trends without statistical significance), except for certain areas in the northwest/southeast where statistically significant positive/negative trends were recorded (Marin et al., 2014), ET values had different dynamics. A relatively recent analysis showed that, after 1961, the parameter's trends have been largely positive and, for the most part, statistically significant (Croitoru et al., 2013a). Although based on this reasoning it can be indirectly deduced that, in Romania, the CWB evolved towards deficit values, this hypothesis is uncertain considering that, to date, no concrete national statistical analyses have been conducted on this index's dynamics.

Such country-wide analyses are essential for the management of agricultural systems, water resource planning or for adapting ecological systems to future climate change. In fact, many anthropic and natural systems are already vulnerable to CWB changes. For instance, it was proven that agricultural crops in several parts of the Romanian Extra-Carpathians region have lately had lower yields against the background of an amplified climatic water deficit (Prăvălie et al., 2014a; Prăvălie et al., 2016b). Other studies also signalled lower streamflow rates in numerous catchments countrywide, especially during summer, when the climatic water deficit has grown constantly over the past decades (Birsan et al., 2014). These examples signal, directly or indirectly, the importance of the CWB as a regulating variable in the dynamics of natural processes or anthropogenic activities. However, in order to analyse similar connexions in future interdisciplinary studies, it will be

necessary to have an in-depth understanding of the index's country-wide pattern changes.

This study aims to analyse the spatial and temporal dynamics of the CWB for Romania's entire territory, in relation to the changes of P and ET constituting parameters between 1961 and 2013. To the best of our knowledge, this is the first study to conduct a country-wide analysis on CWB variability, annually, seasonally and for the growing seasons of two of the country's key agricultural crops. In addition to the CWB analysis, our approach also aims to generate new results on P and ET dynamics for the three time scales (e.g. assessment of P variability rates recorded at the considered weather stations, instead of simply analysing trend types – positive, negative or stationary, analysed in certain studies, or the first ever analysis of ET dynamics at many weather stations), so far unexplored in previous studies. At the same time, this paper also attempts to deliver new results on the response of CWB dynamics on atmospheric circulation on a large scale, by analysing possible connections between this index's interannual variability and that of certain European and global teleconnection indices.

2. Materials and methods

2.1. Study area

With an area of almost 240,000 km^2, Romania is the largest country in Southeastern Europe. The country's landform types are relatively equally distributed between mountains (the Carpathians, 31% of the country's area), hills and tablelands (33%) and lowlands (plains and meadows, 36%), and range altitudinally from 0 to 2544 m a.s.l. (Fig. 1a). Its particular geomorphology and position within the continent induce certain well-defined climatic features.

Thus, western and central regions are dominated by ocean influences and thus are wetter and colder in the summer season, and wetter and milder during winter, while eastern areas, dominated by continental influences, are more extreme in terms of temperature (hotter in summer and colder during winter) and also drier (Sandu et al., 2008). However, some authors claim that the region which receive the most oceanic influences in Romania, especially during westerly circulation, is covering the northern part of Romania due to the lack of mountain barrier (Apostol and Sfîcă, 2013; Sfîcă et al., 2015). The main driver of these complex regional features consists of the Carpathians Mountains (Fig. 1b), which act as a barrier in the way of moist western oceanic air masses and dry eastern continental air advections (but also generate thermal differences, impending cold air advection from the east to be advected in the central and western side of the country) (Apostol and Sfîcă, 2013). In the mountains, the climate is greatly influenced by altitude, slope exposure and the source of air masses advection (Croitoru et al., 2013a). Several other climate features can also be distinguished. Romania's southwestern region, which is under Mediterranean influences, is very warm during summer and has mild and wet winters. Baltic and Scandinavian influences are felt in the northwestern region, which is generally colder and wetter than other regions of the country. Similarly to eastern areas, southeastern regions are exposed to continental influences (responsible for lower winter temperatures and higher summer temperatures, due to the movement of cold continental air masses from the Eurasian region during winter, and of warm tropical or continental air during summer), as well as to Black Sea influences, which plays a moderating role especially on the coastline, where temperatures are higher in winter and lower in summer, compared to Dobrogea inland territories (Prăvălie et al., 2016a).

In terms of the main climatic parameters, mean multiannual temperatures range between 11 and 12 °C in the south, and go below 1 °C in mountainous regions, while precipitation values range from ~300–400 mm in the east/southeast to over 1300 mm in the Carpathians (Fig. 2). In terms of multiannual ET values, they range from < 500 mm in the mountain area to > 800 mm in the Extra-Carpathians region, in the country's southern and southeastern regions (Fig. 2). As such, the highest climatic water deficit (precipitation minus evapotranspiration) can indirectly be identified in the southeast, and the highest surplus in mountainous regions, as a study confirmed a multiannual humidity deficit of ~ − 400 mm, and humidity surplus of over 600–700 mm in these two extreme Romanian regions (Paltineanu et al., 2007). These values are consistent with our countrywide processed and mapped data (Fig. 2).

The analysis of the weather stations' data recorded between 1961 and 2013 points to a dynamic state of the climatic water balance index both annually and seasonally. Annually, the index ranges from − 516.7 mm in the east (Sulina station) to 715.2 mm in the central southwestern region (Obarsia Lotrului) (Table 1, Fig. 1), which reveals a CWB value amplitude of over 1200 mm on Romanian territory. Seasonally, CWB values range from 21 mm (Sulina) to 213 mm (Obarsia Lotrului) in the cold season (winter), and from − 325.7 mm (Gura Portitei) to 227.3 mm (Balea Lac) in the warm season (summer). There are however significant variations in transitional seasons as well – from − 146.4 mm (Sulina) to 174.4 mm (Balea Lac) in spring, and from − 76 mm (Sulina) to 180.3 mm (Obarsia Lotrului) in autumn (Table 1, Fig. 1). A high spatio-temporal CWB variability was also found for the country's two most important agricultural crops (maize, April–October, and wheat, October–June) in terms of cultivated areas (Croitoru et al., 2013a), considering wide value ranges for maize (− 523.4…474.8 mm) and wheat (− 247.2…558.2 mm) growing seasons (Table 1).

The analysis of spatio-temporal CWB variability and trends is particularly important in Romania, considering the country's immense agricultural potential, which is however highly dependent on humidity conditions, given the acute country-wide lack of irrigation systems – e.g. only ~180,000 ha in 2013, compared to ~3.2 mil ha in 1989 (Rusu and Simion, 2015). According to the CORINE Land Cover database (CLC, 2012), ~57% (~13.6 mil ha) of the country's territory is covered by agricultural lands (arable land, vineyards, orchards, pastures and hayfields), which are mainly located in Extra-Carpathians region (~8.3 mil ha, 61% of the total agricultural lands), where the climatic water deficit is at its highest point nationally (Table 1, Fig. 1). Unirrigated arable lands account for 64% (~8.7 mil ha) of the total agricultural lands and are mainly located in Romania's Extra-Carpathian (~6 mil ha, 70% of the total arable lands) and Intra-Carpathian (~2.3 mil ha, 26%) regions (Fig. 1). These arable lands largely consist of maize and winter wheat crops. The analysis of CWB changes is also essential in terms of other economic metrics such as water resource management for meeting water demands of human settlements. Considering the large number of cities (settlements with the most diverse water requirements) throughout the three Romanian regions (165 in the Extra-Carpathians region, 45% of the 367 Romanian cities, 109/30% in the Carpathians area, and 93/25% in the Intra-Carpathians region), this study is also indirectly relevant for highlighting water availability changes across these anthropic systems of the country.

2.2. Climate data

For the analysis of CWB dynamics (including its constituting parameters) and of the relationship between the indicator and the atmospheric circulation on a large scale, two sets of climatic data were used – weather station and teleconnection indices data.

2.2.1. Weather station data

The analysis of CWB index trends and of its constituting parameters was based on mean daily values (subsequently computed as monthly values) for temperature (°C), precipitation (mm), relative air humidity (%) and sunshine duration (hours), extracted for 70 weather stations uniformly distributed throughout Romania's main landforms – plains, plateaus, hills and mountains (Fig. 1a, b). The data covered 53 years homogenously and continuously (1961–2013) and were extracted (exactly in the geographic coordinates of the 70 weather stations) from the ROCADA climatic dataset (Dumitrescu and Birsan, 2015), provided as a

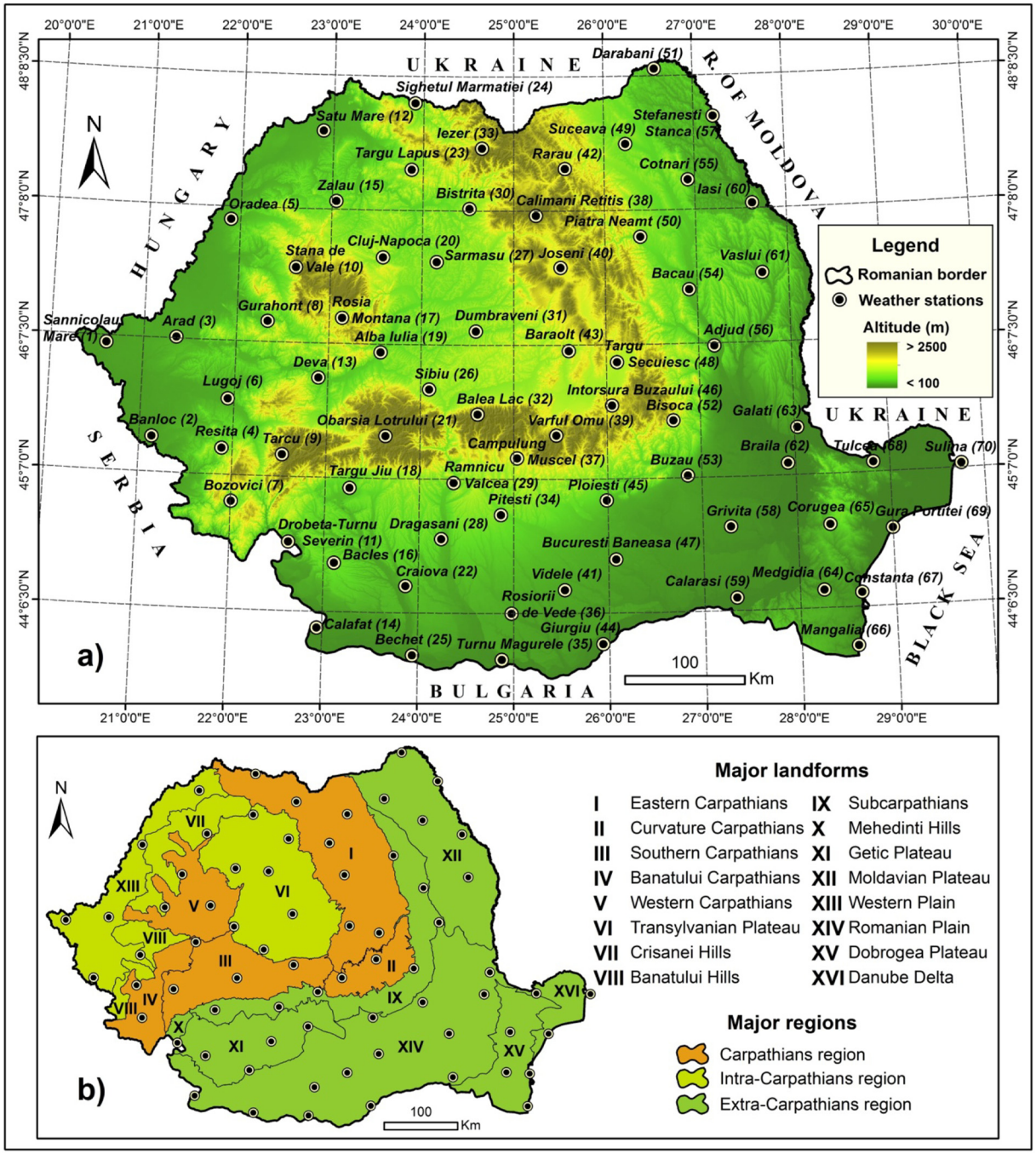

Fig. 1. Location of weather stations analysed in Romania considering altitude (a) and the major grographical regions/landforms (b).

grid database by the National Meteorology Administration (Birsan and Dumitrescu, 2014). As data on wind speed (m/s) were not yet available in the ROCADA dataset, but were necessary for computing evapotranspiration and, implicitly, the water balance index, they were extracted from WorldClim database, version 2.0 (Fick and Hijmans, 2017), as mean multiannual monthly values. Considering the high number of weather stations, distributed in areas with various climatic (drier or more humid, hotter or colder, more or less subjected to various influences of the atmospheric circulation) and geomorphological (depressions or peaks, plains or mountains, low or high altitudes – for this last instance, weather station location differences range from 3 m, Sulina, to 2505 m, Varful Omu) conditions (Table 1), it can be concluded that this study is representative for the country's entire territory and generally for all of its environmental conditions.

2.2.2. Teleconnection indices data

In order to evaluate the influence of large-scale mechanisms of atmospheric circulation on CWB changes, we have selected a couple of teleconnection indices that are recognized for their effect on climatic conditions at European scale. The following indices were used: North Atlantic Oscillation (NAO), Arctic Oscillation (AO), Scandinavian Pattern (SP), Atlantic Multi-Decadal Oscillation (AMO), Quasi-Biennial Oscillation (QBO), Madden Julien Oscillation (MJO), East Atlantic (EA) and East Atlantic-Western Russia (EAWR). Additionally, the possible impact of solar activity was explored using solar flux data (SF). All these teleconnections, as well as solar activity, are known as elements that drive climate conditions in the Euro-Atlantic region, and their impact was analysed in numerous climate studies (Knight et al., 2006; Barriopedro et al., 2008; Zampieri et al., 2017; Salmaso, 2012;

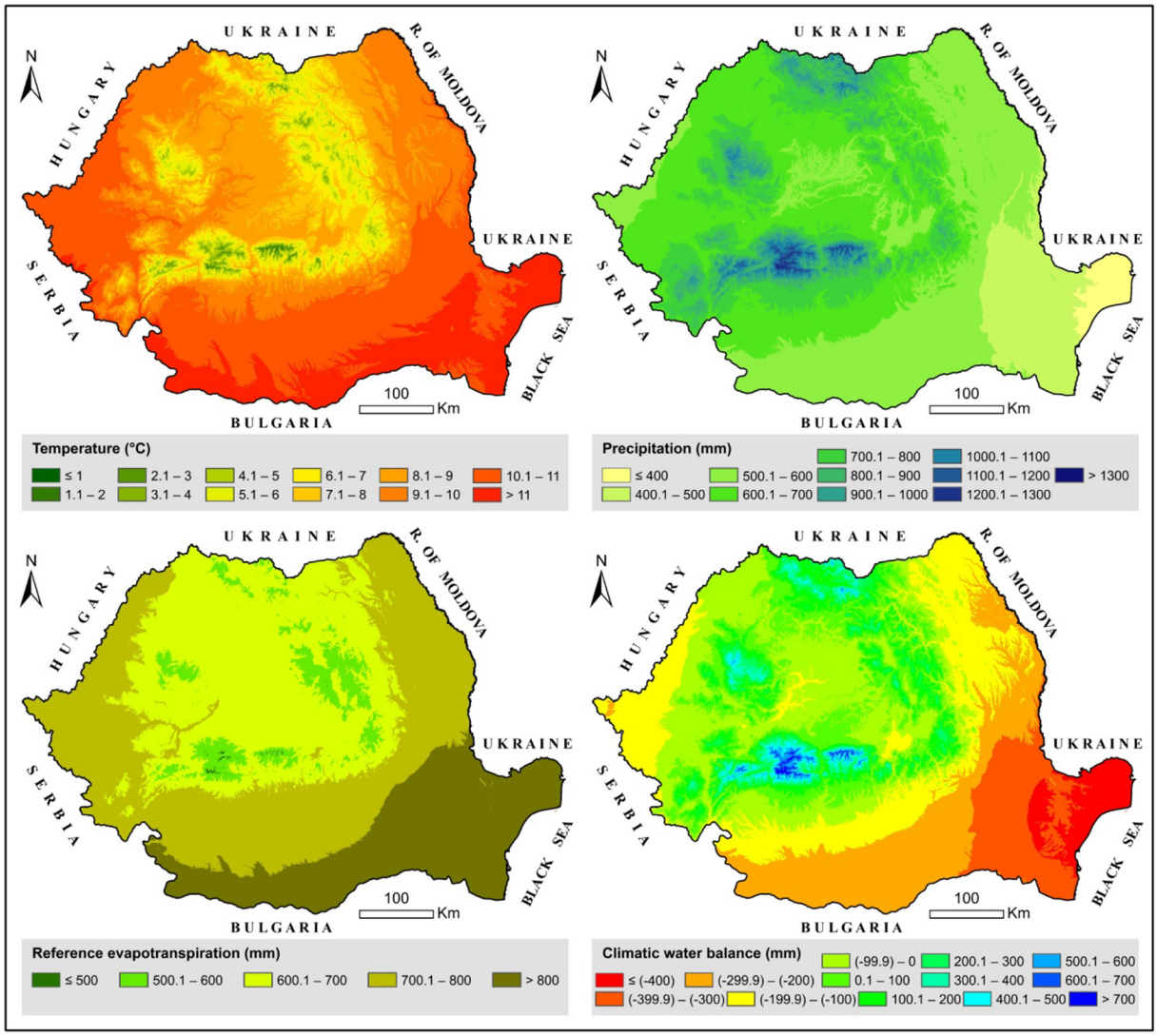

Fig. 2. Spatial distribution of mean multiannual values (1961–2013) for temperature, precipitation, reference evapotranspiration and climatic water balance in Romania.

Casanueva et al., 2014; Irannezhad et al., 2014; Niu et al., 2014; Irannezhad et al., 2015; Sfică et al., 2017).

The 1961–2013 data for these indices were collected from the Climate Prediction Center (NAO, AO, SP, EA, EAWR, MJO) and the Physical Division Science (QBO), from NOAA (NOAA, 2017a, 2017b). Enfield et al. (2001) and the National Research Council of Canada (NRCA, 2017) were used for the AMO database and solar flux (SF), respectively. Monthly values were available for each index, but for our analysis the data was computed for the same seven temporal scales as for CWB.

2.3. Methods

The entire analysis of CWB trends and of the possible influences of the atmospheric circulation on the index's dynamics was conducted in seven main phases, i.e. monthly climatic data calculation, reference evapotranspiration computation, climatic water balance calculation, individual weather stations trend detection, net changes investigation, average weather stations trend detection and teleconnection indices – CWB statistical relation analysis.

2.3.1. Monthly climatic data calculation

Based on daily values of the parameters extracted from the ROCADA grid database (which has a spatial resolution of 0.1° or ~11 km), the mean (temperature and air humidity) and total (precipitation and sunshine duration) monthly values were computed for each year in the 1961–2013 interval. The computations and extraction of monthly climatic values were performed using CDO software-sourced computation modules (CDO, 2015). The software features a series of specific operators for time data series, which can help extract and process grid-type multi-temporal data, like the ones in the RODACA database. Also, ArcGIS 10.1 (ESRI, 2012) was used for extracting multiannual monthly wind values from the WorldClim database (GeoTIFF data at a resolution of 30″ or ~1 km), available for the period 1970–2000 (Fick and Hijmans, 2017). Although the data does not have the same spatial and temporal formats as the ROCADA data, it was integrated into the analysis because we considered that computing monthly evapotranspiration values using the available data would be more accurate than estimating the parameter without it.

2.3.2. Reference evapotranspiration computation

The reference evapotranspiration (ET_o) was computed using the FAO-56 Penman-Monteith (PM) method (Allen et al., 1998). In this respect, the ET_o calculator 3.2 software was used for computing the ET_o (Raes, 2012). This method has proven to provide the most accurate estimation of atmospheric evaporative demand (ET_o) under a variety of

Table 1
Geographic coordinates and mean multiannual climatic water balance values (1961–2013) at the analysed weather stations (*A* annual, *W* winter, *Sp* spring, *Su* summer, *Au* autumn, *Apr–Oct* maize growing season, *Oct–Jun* wheat growing season).

No.[1]	Weather stations	Latitude (N)	Longitude (E)	Alt. (m)	Climatic water balance (mm)						
					A	W	Sp	Su	Au	Apr–Oct	Oct–Jun
1	Sannicolau Mare	46°04′17″	20°36′06″	86.2	−226.4	76.0	−88.3	−207.8	−6.3	−320.7	−39.6
2	Banloc	45°22′58″	21°08′11″	84.6	−161.5	95.0	−75.4	−185.7	4.6	−279.3	1.2
3	Arad	46°08′01″	21°21′13″	117.8	−164.3	83.9	−72.0	−180.9	4.7	−270.0	−1.3
4	Resita	45°18′52″	21°53′13″	280.5	65.4	128.0	−5.6	−104.0	47.0	−105.1	157.6
5	Oradea	47°02′09″	21°53′45″	137.2	−163.3	81.6	−81.4	−174.6	11.1	−267.3	−11.5
6	Lugoj	45°41′12″	21°56′00″	124.3	−51.6	112.2	−44.8	−155.2	36.2	−197.7	79.2
7	Bozovici	44°55′06″	22°00′22″	257.2	−9.1	113.0	−23.0	−125.5	26.4	−150.6	106.7
8	Gurahont	46°16′45″	22°20′00″	178.2	4.2	100.5	−29.3	−106.7	39.7	−131.0	96.1
9	Tarcu	45°16′52″	22°31′58″	2186.0	391.6	141.8	75.8	76.0	98.0	180.6	338.7
10	Stana De Vale	46°41′23″	22°37′24″	1109.2	448.7	173.4	87.6	76.7	111.0	174.1	408.2
11	Drobeta-Turnu Severin	44°37′35″	22°37′34″	78.2	−171.7	106.2	−63.6	−229.6	15.3	−308.3	19.9
12	Satu Mare	47°43′17″	22°53′14″	124.2	−62.7	99.1	−58.3	−136.7	33.2	−198.1	56.5
13	Deva	45°51′54″	22°53′56″	241.2	−82.4	73.6	−60.2	−120.4	24.6	−173.7	17.6
14	Calafat	43°59′06″	22°56′46″	62.2	−293.9	79.3	−92.0	−269.9	−11.3	−394.9	−63.0
15	Zalau	47°11′42″	23°02′48″	296.2	−43.5	79.6	−44.0	−101.3	22.2	−149.0	52.5
16	Bacles	44°28′34″	23°06′47″	315.0	−110.4	103.7	−41.7	−191.7	19.3	−250.5	48.7
17	Rosia Montana	46°19′03″	23°08′21″	1197.2	141.5	105.2	17.0	−34.8	54.1	−12.8	179.2
18	Targu Jiu	45°02′26″	23°15′37″	205.5	4.0	123.9	−29.2	−145.1	54.4	−167.2	120.6
19	Alba Iulia	46°03′50″	23°33′48″	246.9	−156.5	44.5	−68.0	−136.4	3.4	−206.2	−40.0
20	Cluj-Napoca	46°46′40″	23°34′17″	411.3	−103.5	60.9	−59.1	−107.1	1.8	−173.7	0.0
21	Obarsia Lotrului	45°26′08″	23°37′51″	1350.0	715.2	213.0	157.7	164.2	180.3	388.0	558.2
22	Craiova	44°18′37″	23°52′01″	193.2	−208.3	83.9	−75.1	−216.4	−0.7	−319.7	−19.0
23	Targu Lapus	47°26′23″	23°52′20″	365.0	124.5	141.0	−6.6	−77.6	67.7	−78.1	196.1
24	Sighetul Marmatiei	47°56′21″	23°54′16″	276.3	225.7	141.3	6.8	−34.1	111.7	11.2	237.7
25	Bechet	43°47′23″	23°56′39″	37.2	−300.2	70.8	−96.5	−258.3	−16.2	−388.6	−77.8
26	Sibiu	45°47′22″	24°05′29″	444.3	−36.3	56.7	−45.8	−68.5	21.3	−106.7	25.1
27	Sarmasu	46°44′51″	24°09′35″	400.2	−83	65.6	−54.0	−113.6	19.0	−167.1	15.5
28	Dragasani	44°39′56″	24°14′14″	281.4	−128.9	86.4	−60.6	−170.1	15.4	−240.7	16.6
29	Ramnicu Valcea	45°05′20″	24°21′46″	238.3	−23.5	87.7	−32.1	−113.9	34.8	−142.1	73.9
30	Bistrita	47°08′57″	24°30′50″	367.2	58.1	100.4	−21.7	−72.1	51.5	−88.1	121.7
31	Dumbraveni	46°13′40″	24°35′30″	319.1	−42.8	55.7	−39.4	−80.2	21.1	−114.2	29.0
32	Balea Lac	45°36′14″	24°36′53″	2071.2	712.4	134.9	174.4	227.3	175.8	474.8	511.7
33	Iezer	47°36′09″	24°38′56″	1787.0	509.7	157.5	111.0	94.0	147.2	248.2	425.3
34	Pitesti	44°50′56″	24°51′58″	317.2	−82.4	82.2	−49.0	−136.6	21.0	−190.0	36.2
35	Turnu Magurele	43°45′37″	24°52′42″	31.6	−276.8	72.5	−95.0	−235.8	−18.5	−363.9	−72.8
36	Rosiorii De Vede	44°06′26″	24°58′43″	103.4	−277.6	70.4	−94.9	−234.4	−18.7	−364.6	−75.6
37	Campulung Muscel	45°16′29″	25°02′12″	680.0	172.6	115.7	21.5	−28.8	64.2	4.0	202.1
38	Calimani Retitis	47°05′53″	25°14′46″	2021.0	292.3	69.6	70.9	87.2	64.6	173.0	235.5
39	Varful Omu	45°26′45″	25°27′24″	2505.0	243.0	95.9	28.2	56.9	62.0	112.5	193.9
40	Joseni	46°42′21″	25°30′45″	751.3	−10.3	47.5	−33.1	−38.7	14.0	−68.3	27.3
41	Videle	44°16′58″	25°32′13″	107.0	−251.2	72.7	−90.6	−219.9	−13.4	−341.8	−62.1
42	Rarau	47°26′58″	25°34′05″	1536.0	94.9	34.0	4.8	36.4	19.7	48.4	74.6
43	Baraolt	46°04′51″	25°35′45″	510.0	−75.7	53.4	−55.2	−78.8	4.9	−133.9	−6.0
44	Giurgiu	43°52′31″	25°55′58″	24.8	−258.9	82.5	−92.2	−242.2	−7.0	−365.1	−58.3
45	Ploiesti	44°57′21″	25°59′15″	178.2	−129	72.9	−69.2	−140.8	8.1	−221.0	−2.6
46	Intorsura Buzaului	45°40′06″	26°03′24″	708.2	52.0	50.5	−13.2	−10.1	24.8	−11.9	64.2
47	Bucuresti Baneasa	44°30′38″	26°04′41″	91.2	−210.1	75.3	−81.8	−203.6	0.0	−304.4	−35.7
48	Targu Secuiesc	45°59′34″	26°06′54″	570.0	−67.3	40.8	−36.8	−74.2	2.9	−111.1	2.3
49	Suceava	47°37′58″	26°14′26″	353.2	−46.8	40.6	−37.2	−54.3	4.1	−97.8	7.1
50	Piatra Neamt	46°56′01″	26°23′22″	361.6	−77.7	36.5	−45.7	−67.8	−0.7	−121.4	−9.1
51	Darabani	48°11′42″	26°34′25″	260.2	−145.7	40.3	−65.5	−119.6	−0.9	−194.8	−46.3
52	Bisoca	45°32′56″	26°42′37″	851.3	28.7	58.2	−0.5	−51.1	22.1	−53.8	77.5
53	Buzau	45°07′58″	26°51′06″	98.3	−314.2	40.2	−106.0	−214.9	−33.5	−353.4	−122.6
54	Bacau	46°33′28″	26°53′48″	175.2	−173.6	40.9	−70.6	−136.0	−7.9	−217.9	−52.2
55	Cotnari	47°21′30″	26°55′32″	290.2	−168.4	39.9	−71.6	−126.4	−10.3	−214.7	−55.4
56	Adjud	46°06′17″	27°10′13″	102.4	−210.4	47.7	−76.3	−175.2	−6.6	−264.1	−65.5
57	Stefanesti Stanca	47°49′56″	27°13′11″	111.2	−191.6	44.3	−90.3	−140.1	−5.5	−240.8	−73.1
58	Grivita	44°44′27″	27°17′41″	51.1	−334.5	48.2	−112.9	−241.2	−28.6	−384.9	−127.2
59	Calarasi	44°12′21″	27°20′18″	19.9	−334.5	54.6	−114.1	−258.0	−17.0	−396.1	−117.9
60	Iasi	47°09′48″	27°37′38″	75.7	−222.9	45.5	−93.5	−161.2	−13.7	−273.5	−81.3
61	Vaslui	46°38′46″	27°42′52″	117.2	−243.5	44.3	−95.3	−178.2	−14.3	−292.5	−89.0
62	Braila	45°12′24″	27°55′11″	15.7	−390.9	40.6	−126.3	−264.9	−40.3	−428.4	−162.9
63	Galati	45°28′23″	28°01′56″	70.3	−351.1	49.3	−115.9	−252.8	−31.7	−400.8	−132.5
64	Medgidia	44°14′36″	28°15′05″	70.7	−393.2	45.4	−115.2	−281.9	−41.5	−440.7	−154.8
65	Corugea	44°44′04″	28°20′31″	220.4	−395.9	39.5	−119.7	−270.3	−45.4	−429.4	−166.6
66	Mangalia	43°48′58″	28°35′15″	7.2	−371.7	39.1	−93.6	−284.5	−32.7	−417.6	−135.6
67	Constanta	44°12′50″	28°38′44″	14.0	−440.1	38.4	−114.9	−307.2	−56.4	−478.0	−177.4
68	Tulcea	45°11′26″	28°49′27″	5.6	−422.9	40.6	−133.4	−285.8	−44.3	−458.2	−186.7
69	Gura Portitei	44°41′23″	28°59′56″	3.2	−495.6	27.9	−133.3	−325.7	−64.5	−515.1	−220.2
70	Sulina	45°08′54″	29°45′32″	3.0	−516.7	21.0	−146.4	−315.3	−76.0	−523.4	−247.2

Note: 1 – stations are ordered from west to east, based on increasing longitude coordinate values.

climates and it is widely recommended (Maeda et al., 2011; Fan and Thomas, 2013). The FAO-56 PM method was selected by the Food and Agriculture Organization of the United Nations (FAO), the International Commission on Irrigation and Drainage, and by the American Society of Civil Engineers as the standard procedure for computing ET_o (Vincente-Serrano et al., 2010).

ET_o is defined as the atmospheric evaporative demand from a reference surface consisting of a hypothetical reference crop with a height of 0.12 m, a fixed surface resistance of 70 sm^{-1} and an albedo of 0.23 (Allen et al., 1998; Croitoru et al., 2013a; Fan and Thomas, 2013). The reference surface closely resembles an extensive surface of green grass of uniform height, actively growing, well-watered and completely shading the ground (Allen et al., 1998; Croitoru et al., 2013a). The calculation procedure for ET_o is described in detail in FAO Irrigation and Drainage Paper No. 56 (Allen et al., 1998) and was explained in a large number of studies (Tabari et al., 2012; Croitoru et al., 2013a; Fan and Thomas, 2013; Fan et al., 2016; Feng et al., 2017).

The computation of ET_o using the FAO-56 PM method requires extensive data (usually solar radiation, air temperature, humidity, and wind speed), but is highly flexible when data are lacking, and can deliver reasonable accuracy even if computed with missing data. The more measured meteorological variables are considered to estimate ET_o, the more accurate the results seem to be (Croitoru et al., 2013a). In this study, ET_o was computed based on monthly climatic data – mean air temperature, relative humidity, sunshine duration, and wind speed. Considering that wind speed data was available only on a multiannual monthly time-scale (as it was not available in the ROCADA database, as previously mentioned), we used the same wind speed value of a specific month in each year of the interval 1961–2013. When wind speed values are missing, the ET_o calculator 3.2 software uses a general mean value of 0.5 m/s for areas with light wind, 2.0 m/s for areas with light to moderate wind, 4 m/s for areas with moderate to strong wind, and 5.5 m/s for areas with strong wind, or a value of 2 m/s if no wind values are available within the region, according to the methodology outlined in the Irrigation and Drainage Paper No 56 (Allen et al., 1998). Instead of accepting the default values of the ET_o calculator 3.2 in the case of wind speed estimation, we preferred to use mean multiannual monthly values for each weather station, which provides a better estimation of ET_o than a single universal value for all stations and months of the year would.

2.3.3. Climatic water balance calculation

Monthly climatic water balance (CWB, in mm) values were computed based on the difference between precipitation and reference evapotranspiration ($CWB = P - ET_o$). These monthly values were subsequently summed up in order to obtain annual (the 12 months of the year) and seasonal (winter: December–February; spring: March–May; summer: June–August; autumn: September–November) CWB values, as well as for the growing seasons of the of the country's main agricultural crops, i.e., maize (April–October) and wheat (October–June). Also, the same periods were used for estimating the values of P and ET_o and their trends for the seven time scales. While CWB is easily computable once ET_o values are obtained, it is highly suggestive and complex index, considering the fact it includes two essential climatic parameters (or five, if considering the variables that constitute ET_o) that fundamentally influence the anthropic (especially agricultural) and ecological systems dynamics of a given territory. This climatic approach to the water balance was used in a series of climatic, agro-climatic, hydro-climatic and eco-climatic studies conducted in various regions in Romania (Paltineanu et al., 2007, 2009; Bandoc and Prăvălie, 2015; Prăvălie et al., 2016b, 2016c) and worldwide (Kar and Verma, 2005; Seager et al., 2007; Zhang et al., 2009; Crimmins et al., 2011; Byrne and O'Gorman, 2015).

2.3.4. Individual weather stations trend detection

The non-parametric Mann-Kendall (Mann, 1945; Kendall, 1975) test and *Sen's slope* estimator (Sen, 1968) were used to detect the trends and their magnitudes for the CWB, as well as for P and ET_o (at each weather station), in order to accurately identify the causes of CWB changes by analysing the dynamics of the two constituting parameters separately. The methods, applied in this paper using the *MAKESENS* Excel software (Salmi et al., 2002), are highly recommended by the World Meteorological Organization for identifying trends in hydro-climatic variables and were largely used in many such studies across the globe (Tabari et al., 2012; Croitoru et al., 2013a, 2013b; Fan and Thomas, 2013; Birsan et al., 2014; Prăvălie and Bandoc, 2015; Zhao et al., 2015; Bastia and Equeenuddin, 2016; Fan et al., 2016; Feng et al., 2017; Palizdan et al., 2017). The Mann-Kendall test indicates if a trend is statistically significant, while the *Sen's slope* method gives the sign (increasing or decreasing) and estimates the trend's magnitude. The statistical significance of P trends or indices that include this parameter, like the CWB, is lower than other climatic variables due to its large spatio-temporal variability (Łupikasza et al., 2011; Croitoru et al., 2016b).

Therefore, the CWB trends were assessed considering two statistical significance levels: $\alpha = 0.1$ (significant trends) and $\alpha = 0.05$ (strong significant trends). Therefore, the $\alpha = 0.1$ significance threshold was also taken into account in this paper, similarly to other climatic studies on precipitation dynamics (Łupikasza et al., 2011; Huang et al., 2013; Wong et al., 2015; Ávila et al., 2016; Demaria et al., 2017). Also, in order to emphasize the strong changes or the weak ones in P and ET_o, which explain the CWB dynamics, the trends' statistical significance for the two parameters was evaluated using four levels: $\alpha = 0.1$, 0.05, 0.01, and 0.001. For all analysed cases of the 1961–2013 period, slopes were presented as change per year (mm/yr). Besides the positive/negative trends, this study also considered stationary trends, defined by a slope value of 0.000 (Croitoru et al., 2013b).

2.3.5. Net changes investigation

In addition to the annual rates detected with the Mann-Kendall and *Sen's slope* methods, we deemed it necessary and interesting to analyse the net/total CWB changes over the entire 53-year period. To this end, interpolation procedures were used, which helped synthesize and more accurately interpret the results in a national context. As correlations with terrain altitude were not statistically significant, the spatial distributions of the CWB on the seven temporal scales were derived through ordinary and universal kriging interpolations using the Geostatistical Analyst module featured in the ArcGIS 10.1 software (ESRI, 2012). Universal kriging was applied only for autumn, as its performance was better than ordinary kriging, according to the root mean square errors of the cross-validation procedure (Dobesch et al., 2007; Patriche, 2009). Thus, the data on net changes in the CWB (annual trends multiplied by 53) provided by the 70 weather stations was used for interpolations, and the digital maps were generated at a resolution of 500 × 500 m.

2.3.6. Average weather stations trend detection

In order to synthesize and highlight the overall CWB dynamics nationally and regionally, we considered that a averaging of trend/change values over extensive regions would be highly suggestive for this index. To this end, the annual and net changes of CWB were averaged nationally, in the three major regions (Carpathians, Intra-Carpathian and Extra-Carpathian regions) and in the 16 major Romanian landform units (Posea and Badea, 1984) (Fig. 1b). While in the first two cases the mean values were obtained based on all/a large number of weather stations countrywide/in the three major regions, for the landforms analysis the information was extracted by averaging values obtained from 2 (e.g. Curvature Carpathians) and up to 14 (Romanian Plain) weather stations (Fig. 1b). The exceptions consist of two landform units in which a single station was available – Banatului Hills (Lugoj station) and Mehedinti Hills (Drobeta-Turnu Severin) (Fig. 1b), which is why in these cases only the individual values of the annual trend/net change recorded at that station were extracted.

2.3.7. Teleconnection indices – CWB statistical relation analysis

To simplify the analysis in terms of atmospheric circulation, the first stage of this phase consisted of averaging the CWB data from the 70 weather stations in the country's three major regions: Carpathian, Intra-Carpathian and Extra-Carpathian regions (Fig. 1b). This resulted in three interannual data series that were subsequently statistically correlated with teleconnection indices.

Due to the lack of correlations obtained between CWB and solar activity and Madden-Julien Oscillation, the results for SF and MJO are not shown in the study. Therefore, even if these indices are considered to have an effect on climate elements at European scale (Casanueva et al., 2014; Gray et al., 2010), our results are mainly due to the complexity of the water balance index which integrates data for 5 climate elements, while solar activity only has a clear and limited impact on temperature (Gray et al., 2010). Also, the Madden-Julien Oscillation was found to have an impact especially on the precipitation regime (Casanueva et al., 2014).

To identify the statistical relations between CWB and these teleconnections, we started by applying a correlation test (second stage). Since we did not expect direct simple linear correlations between the analysed elements, we preferred the Spearman correlation test over the Pearson correlation. The Spearman method proved to be the most appropriate considering that several teleconnection indices (AMO, QBO, MJO) did not have a normal distribution, according to the results of the Shapiro-Wilk test (Royston, 1982). Afterwards, the correlation test results were reinforced by a composite analysis (the third working stage), which entailed computing the difference between the upper and lower third CWB values, sorted according to the descended time series of each teleconnection index. This difference was tested with a z-test for difference between means (Wilks, 2011) for teleconnection indices with normal distribution, and with Wilcoxon's test for teleconnection indices with non-normal distribution. The Spearman test and composite analysis results were tested at 0.05 level of significance. The entire analysis was processed using the Excel package and XLSTAT software (XLSTAT, 2017).

3. Results

3.1. Climatic water balance annual changes

The Mann-Kendall and *Sen's slope* methods highlighted intense CWB dynamics (expressed based on changes per year or annual changes) at the 70 weather stations, over the five analysed decades (Fig. 3). Annually, apparent predominantly negative CWB trends were found (63 cases out of the total 70, i.e. 90%), which indicates an overall amplification in the climatic water deficit nationally (Figs. 3a, 4).

However, it was found that this deficit increase is statistically significant in only 10% of analysed stations (Fig. 4), especially in the country's southwestern and southeastern regions, which have clearly become drier in the past half-century (Fig. 3a). Quantitatively, most of the negative trends were identified in the interval $-1.01\ldots-2$ mm/yr, followed by $-0.01\ldots-1$ mm/yr (Fig. 3a). In contrast, it appears some areas in the northwestern region recorded higher humidity values, considering the index's positive trends that indicate CWB dynamics towards the excedent direction.

The separate analysis of constituting parameters P and ET_o delivers interesting explanations regarding the causes of the dynamics recorded over Romania's territory. The overall decrease in CWB values was generated by the almost full-scale evapotranspiration amplification – 99% total positive trends and 86% total significant positive trends, although precipitation had also predominantly positive trends, but only in 57% of cases and with almost non-existent statistical significance (Fig. 4, Table 2). At the same time, annual CWB changes can also be explained based on *Sen's slope* values, generally higher for ET_o compared to P (Table 2).

Seasonally, CWB variability is even more apparent. In winter, changes are generally mixed countrywide, but the negative trends are dominant (found exclusively in the interval $-0.01\ldots-1$ mm/yr) (Fig. 3b), which total 67% of the analysed stations (Fig. 4). The limited cases of statistically significant CWB decreases in the southeast (coastal region, Danube Delta sector) show that this region of the country experienced the strongest dry conditions on this time scale as well (Fig. 3b). The analysis of the dynamics of constituting parameters showed that CWB decreases are due to the overall decrease in precipitation amounts (in 60% of analysed cases) and to the increase in evapotranspiration values (57% overall) (Fig. 4, Table 2). Inversely, the index's increase trends in the cold season are generally due to P increases and to the stationary/negative ET_o trends (Table 2).

In spring, widespread CWB decreases were noticed (87%, mainly found in the interval $-0.01\ldots-1$ mm/yr), except for certain areas in the country's western and northwestern regions, where contrary trends were identified (Figs. 3c, 4). It was found that Romania's Extra-Carpathian regions (southwest, south and southeast) had the entire 14% share of CWB significant negative trends (with changes mainly ranging from -1.01 to -2 mm/yr) (Figs. 3c, 4). These areas are therefore the dryness hotspots in this transitional season. The CWB pattern changes can be explained by the negative changes in precipitation (in over 50% of cases, but generally with no statistical significance), that occurred concomitantly with the exclusive evapotranspiration increase (statistically significant in almost 90% of cases) (Fig. 4, Table 2).

The warm season stands out with almost exclusively negative CWB trends (97%) nationally (Fig. 3d), which are however far less statistically significant (14%) (Fig. 4). While the country's southeastern region remains a hotspot for climatic water deficit increases, it is interesting to note there are other areas in the west and northwest with clear, significant CWB decreases (Fig. 3d). All negative CWB trends (with or without statistical significance) are characterized by rates of up to -2 mm/yr, except for a particular case in the southwest, which reaches -3.5 mm/yr (Fig. 3d). The entire CWB summer variability is accounted for by the overall decreasing P trends (in almost 60% of cases, which are however not statistically significant, except for a single case), and by the exclusive increase of ET_o (statistically significant in 100% of cases) (Fig. 4, Table 2).

Autumn is marked by an almost exclusive increase in humidity conditions countrywide (except for two cases in the southeast), which is however statistically significant only at 11% of analysed weather stations (mainly located in the country's western half) (Figs. 3e, 4). In this season, which is an exception in terms of trends, CWB increases mainly range from 0.01 to 1 mm/yr (Fig. 3e). All these positive trends are the result of P increases (97% of cases, 10% of which are significant positive trends) and ET_o decreases (76% of cases, 21% of which are significant negative trends) (Fig. 4, Table 2).

The two growing seasons are dynamic as well. In the maize growing season, negative CWB trends were found in 86% of cases (approximately equally distributed in the intervals $-0.01\ldots-1$ mm/yr and $-1.01\ldots-2$ mm/yr) (Figs. 3f, 4). The country's southeastern region is yet again a hotspot of drier trends, in terms of statistical significance (Fig. 3f). Interestingly, all these dominant drier trends are the result of positive P trends in 80% of cases (with limited statistical significance), which are however overwhelmingly counterbalanced by positive ET_o trends in terms of cases (100%) and statistical significance (94%) (Fig. 4, Table 2).

In the wheat growing season, the negative CWB trends are even more apparent, in terms of weather station cases (97%) and statistical significance (17%) (Figs. 3g, 4). In this instance, the most noticeable hotspot for the index's decreasing trends (statistically significant, which exceeded -3 mm/yr) is found in the southwest (Fig. 3g). The CWB pattern changes of this growing season is a response to the widespread P decrease (64%, with limited statistical significance) and full-scale ET_o increase (99% overall or almost 80% in terms of statistical significance) (Fig. 4, Table 2).

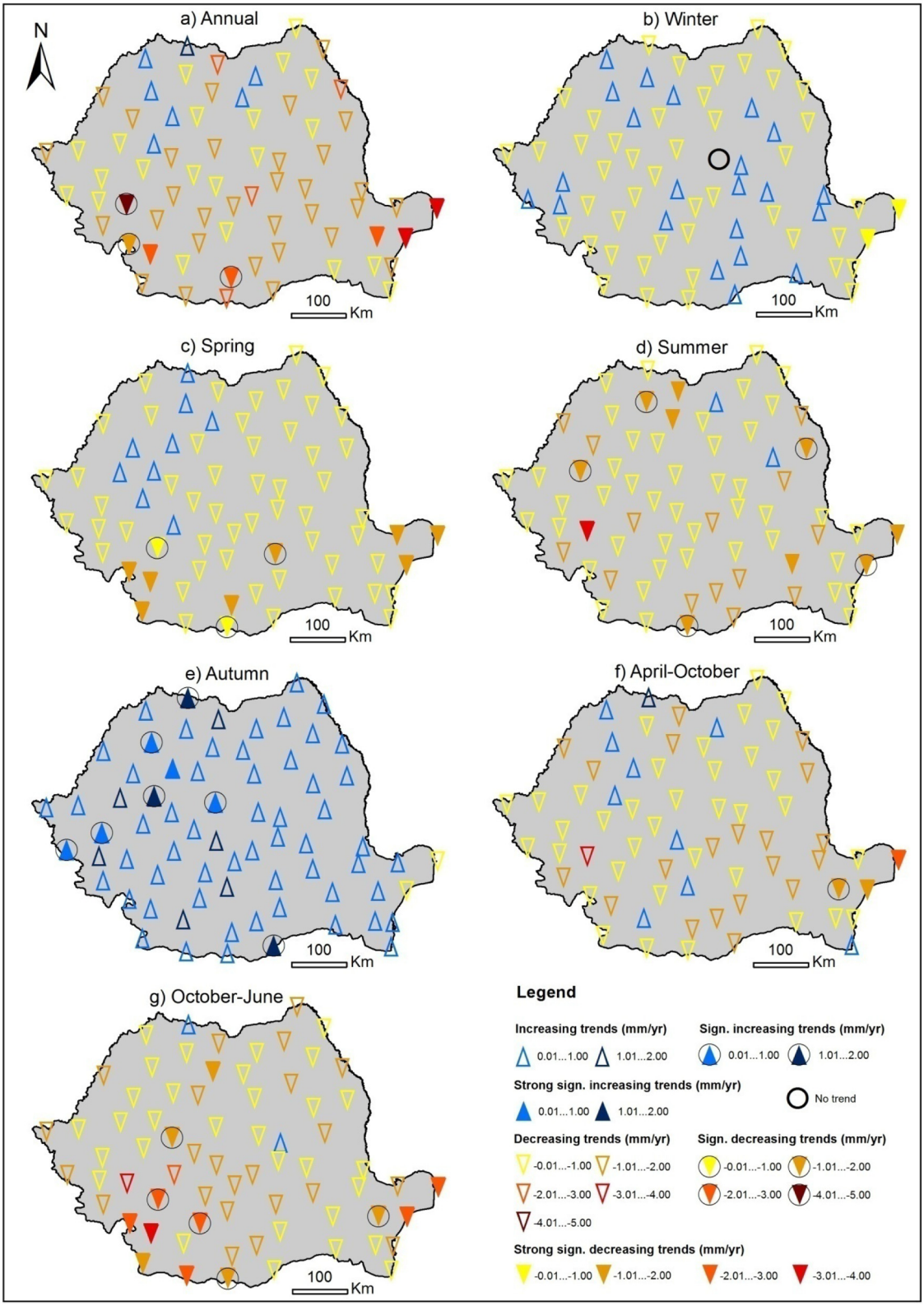

Fig. 3. Climatic water balance trends (direction, magnitude and statistical significance) on the seven temporal scales, in the 1961–2013 period. Note: stationary trends were identified considering a slope value of 0.000.

3.2. Climatic water balance net changes

The analysis of net changes throughout the entire study period highlighted a total amplification of the humidity deficit of up to −236 mm/53 yrs in the country's southwestern region (followed by the southeast, Danube Delta, where the total CWB decrease reached almost −200 mm/53 yrs) annually (Fig. 5a). In contrast, the country's northwest (especially the northwestern/northern extremities of the Carpathian/Intra-Carpathian regions) experienced an overall improvement of humidity conditions, as net positive changes of CWB exceeded the

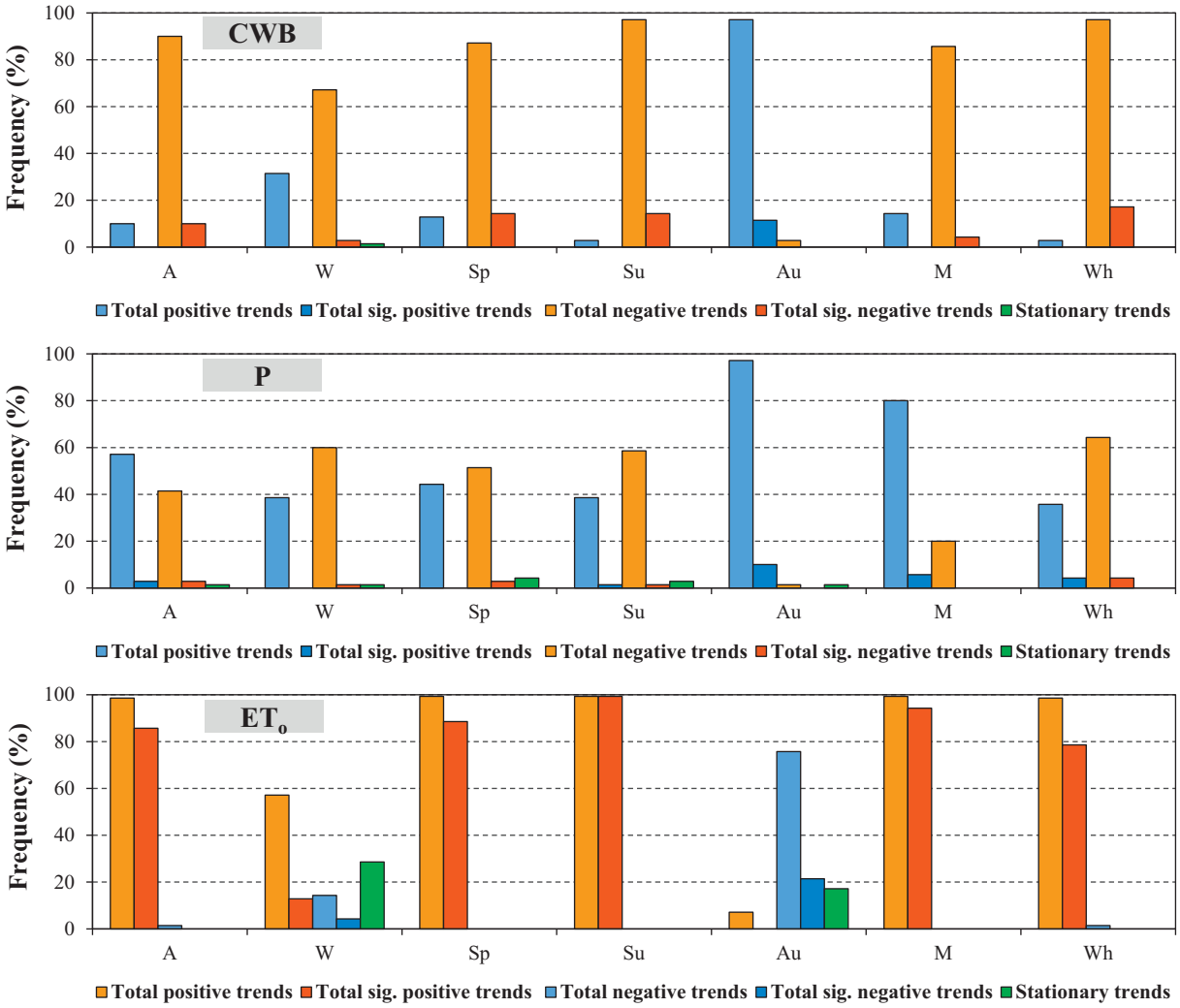

Fig. 4. Relative frequency trends (1961–2013 period) of climatic water balance (CWB), precipitation (P) and reference evapotranspiration (ET_o) on the seven temporal scales (*A* annual, *W* winter, *Sp* spring, *Su* summer, *Au* autumn, *M* maize growing season, *Wh* wheat growing season), according to direction (positive/negative/stationary) and statistical significance (significant/insignificant). Note: for CWB and P, the colours of positive and negative trends were selected in order to highlight climatic changes that consist of increases in humidity (shades of blue) and dryness (shades of orange); for ET_o, the colours were reversed in order to highlight the same reasoning. (For interpretation of the references to colour in this figure legend, the reader is referred to the web version of this article.)

70 mm/53 yrs threshold (Fig. 5a). However, the areas that became wetter are far inferior to most Romanian regions (over 90%) that became drier in the past half-century (Fig. 5h).

Seasonally, some parts of western Romania are remarkable in winter due to a contrary state of affairs, where CWB net positive changes reached a 30 mm/53 yrs peak (Fig. 5b). Inversely, the southeastern region remains a hotspot for net water deficit changes, which in this case reached a national peak, close to −50 mm/53 yrs (Fig. 5b). Although in this season annual CWB trends were interpreted as generally mixed, the areas that became drier (analysed based on spatial interpolation of climatic data) are noticeably superior (almost 70% of the country) compared to those that became wetter (Fig. 5h).

Net climatic water deficit increases can also be noticed in spring especially in Extra-Carpathian regions, with maximum values in the southwest (almost −80 mm/53 yrs) and southeast (almost −70 mm/53 yrs) (Fig. 5c). These increases cover almost 90% of the country's territory (Fig. 5h). While another net amplification of the humidity deficit was also found in summer, it is much more intense (it even exceeds −180 mm/53 yrs in the southwest) and covers a wider spatial scale (in the three major regions of the country) (Fig. 5d). In terms of percentages, the net water deficit increases in the warm season are ampler and cover Romania's territory almost entirely (Fig. 5h). At the opposite pole, the net increase in humidity surplus in autumn (which exceeds 80 mm/53 yrs in the northwest) also covers the country's territory almost entirely (Fig. 5e, h).

The growing seasons of the two agricultural crops were marked by maximal net increases in the humidity deficit close to −200 mm/53 yrs (maize growing season, in the southwest) and −180mm/53 yrs (wheat growing season, also in the southwest) (Fig. 5f, g). The magnitude of the total CWB decrease is therefore surprising, as during these seasons over 95% of Romanian lands became drier over the past five decades (Fig. 5h).

3.3. Mean annual and net changes of the climatic water balance across the country

By averaging CWB changes in large spatial areas in Romania it was found that, annually, annual trends/total changes range from −2.68 mm/yr/−142.25 mm/53 yrs (Danube Delta) to −0.14/yr/−7.44 mm/53 yrs (Western Carpathians), when considering the detailed landform units (Table 3). With regard to the major regions, the Extra-Carpathians experienced the amplest mean deficit dynamics, which reached −1.46 mm/yr/−77.43 mm/53 yrs (Table 3). Overall, Romania recorded a mean increase of the climatic water deficit of

Table 2
Precipitation and reference evapotranspiration annual trends (slopes and their statistical significance in the 1961–2013 period) at the weather stations (*A* annual, *W* winter, *Sp* spring, *Su* summer, *Au* autumn, *Apr–Oct* maize growing season, *Oct–Jun* wheat growing season).

No.[1]	Precipitation (mm/yr)							Reference evapotranspiration (mm/yr)						
	A	W	Sp	Su	Au	Apr–Oct	Oct–Jun	A	W	Sp	Su	Au	Apr–Oct	Oct–Jun
1	0.00	−0.25	−0.12	−0.25	0.68	0.16	−0.71	0.87	0.00	0.31	0.74*	−0.01	0.97+	0.37
2	0.70	0.41	−0.15	0.15	0.71	0.52	−0.25	0.70+	0.01	0.33*	0.62**	−0.15	0.71+	0.42
3	0.90	−0.14	0.17	−0.01	0.73	0.61	0.05	1.01*	0.08	0.37+	0.75**	−0.08	1.00*	0.65+
4	0.61	0.49	0.21	−0.60	0.88	0.08	−0.19	0.52	−0.03	0.25	0.54*	−0.13	0.61	0.29
5	−0.01	−0.21	0.12	−0.42	0.38	0.01	−0.87	1.08*	0.00	0.35+	0.78**	0.00	1.10*	0.61*
6	0.12	0.32	−0.01	−0.14	0.61	−0.03	−0.50	0.62	−0.01	0.28+	0.59*	−0.16	0.71+	0.38
7	−0.12	−0.05	−0.16	−0.86	0.51	−0.32	−0.83	0.78+	0.01	0.31+	0.58*	−0.11	0.87*	0.34
8	0.65	0.06	0.47	−0.42	0.84	0.44	0.34	1.06**	0.00	0.29+	0.83***	0.00	1.02**	0.64**
9	−3.60+	−0.22	−0.43	−2.64*	0.14	−2.76	−2.70+	−0.08	−0.27**	0.10	0.51+	−0.28+	0.35	−0.07
10	0.01	−0.21	0.47	−0.52	0.74	0.22	−0.02	1.08**	0.02	0.37*	0.84***	−0.01	1.04**	0.65**
11	−0.61	−0.33	−0.77	−0.24	0.23	0.08	−1.52	0.94*	0.08	0.42*	0.67*	−0.19+	0.69+	0.58*
12	1.72	0.24	0.29	0.10	0.67	1.23	0.19	1.03*	0.00	0.32*	0.84***	0.00	1.16**	0.68**
13	0.80	−0.27	0.46	0.16	0.37	0.90	0.05	0.87**	0.02	0.26+	0.69**	−0.01	0.81*	0.47*
14	0.11	−0.19	−0.67	0.24	0.33	0.74	−1.05	1.08*	0.09	0.44**	0.73*	−0.13	0.87*	0.65*
15	1.35	0.09	0.37	−0.06	0.81+	1.00	0.38	1.21**	0.00	0.38*	0.86***	−0.01	1.10**	0.70**
16	−1.21	−0.66	−1.19*	−0.14	0.36	0.05	−2.30*	0.85*	0.02	0.38*	0.66**	−0.20*	0.68*	0.57*
17	1.74	−0.04	0.90	0.24	1.04+	1.70	0.39	1.02**	0.03	0.32*	0.77***	−0.01	1.00**	0.56*
18	−0.50	−0.23	−0.67	0.29	0.37	0.42	−1.56	0.56	0.00	0.26+	0.57*	−0.15*	0.48+	0.34
19	0.13	−0.28	0.00	0.06	0.41	0.30	−0.59	1.33***	0.00	0.40**	0.99***	0.00	1.30***	0.80**
20	1.89+	0.13	0.44	0.43	0.89*	1.48	0.74	1.13***	0.00	0.37**	0.81***	0.00	1.08**	0.68**
21	−1.23	−0.07	0.17	−0.85	0.30	−0.09	−1.66	0.44	−0.02	0.18	0.53**	−0.15+	0.56	0.26
22	0.54	−0.08	−0.08	0.40	0.73	1.03	−0.08	0.89*	0.02	0.40*	0.61*	−0.17+	0.67*	0.54*
23	0.93	0.21	0.46	−0.54	0.76	0.52	0.15	1.05**	0.00	0.36*	0.77***	0.00	1.06**	0.67**
24	2.35+	−0.03	0.89	0.45	1.37+	2.45*	1.31	0.99**	0.00	0.35*	0.75***	0.00	0.97**	0.64**
25	−0.68	−0.29	−0.17	−0.01	0.03	0.61	−1.21	1.14**	0.08	0.43**	0.79**	−0.11	0.97**	0.63*
26	0.30	−0.18	0.00	0.63	0.35	0.78	−0.50	0.77**	0.01	0.20	0.67***	−0.12	0.79**	0.50*
27	0.35	0.00	0.21	−0.01	0.62	0.35	−0.10	1.11***	0.00	0.38**	0.86***	0.00	1.16***	0.77***
28	−0.65	−0.35	−0.66	−0.44	0.42	−0.17	−1.59	0.87*	0.06	0.31+	0.57*	−0.17*	0.58+	0.46+
29	−0.63	0.13	−0.44	−0.19	0.47	−0.09	−1.03	1.15**	0.02	0.42**	0.69**	−0.08	0.98**	0.67**
30	−0.70	0.15	0.49	−1.05	0.00	−0.77	−0.99	1.16***	0.00	0.37**	0.91***	0.00	1.20***	0.72**
31	0.17	−0.09	0.04	0.04	0.73+	0.31	−0.08	1.03***	0.00	0.24+	0.86***	−0.02	1.05***	0.52*
32	0.34	0.08	0.10	−0.12	1.07	0.98	−0.80	0.45	0.00	0.17	0.48*	−0.19+	0.48+	0.12
33	−0.61	−0.42	0.23	−0.90	1.02	0.01	−0.85	1.06**	0.07	0.32*	0.79***	−0.10	0.91**	0.61*
34	1.14	−0.07	0.00	0.41	0.94+	1.56	−0.30	1.24***	0.03	0.45**	0.76**	−0.15*	1.00**	0.67**
35	−1.02	−0.31	−0.45	−0.42	0.52	0.34	−0.98	1.14**	0.00	0.45**	0.93**	−0.16	1.06**	0.55*
36	−0.97	−0.26	−0.57	−0.27	0.49	0.31	−0.90	1.39**	0.00	0.61***	0.88**	−0.15	1.28**	0.73**
37	−0.17	−0.22	−0.19	0.00	0.73	0.80	−0.74	0.84**	0.05	0.34*	0.68**	−0.14+	0.77**	0.53**
38	0.32	−0.09	0.14	−0.13	0.53	0.70	−0.45	0.77+	−0.03	0.28*	0.83***	−0.24+	0.82*	0.44
39	−1.05	0.01	−0.09	−0.42	0.45	−0.24	−0.80	0.46	−0.03	0.27	0.55*	−0.24+	0.61	0.24
40	0.35	−0.05	−0.20	0.31	0.48	0.54	−0.06	1.03**	0.00	0.31*	0.74***	−0.01	0.91**	0.53*
41	−0.20	0.11	−0.27	−0.51	0.51	0.13	−0.19	1.48**	0.00	0.59**	0.87**	−0.09	1.29**	0.69**
42	1.54	0.04	−0.19	1.01	0.63	1.41	0.26	1.38***	0.08	0.44**	0.91***	−0.02	1.21**	0.92**
43	0.34	−0.05	0.13	0.05	0.48	0.59	0.09	0.91**	0.00	0.33*	0.77***	−0.02	0.95**	0.57*
44	−0.08	0.43	−0.42	−0.56	0.77	−0.07	0.09	1.05*	0.02	0.48*	0.72*	−0.22*	0.93*	0.49
45	0.01	0.13	−0.50	−0.01	0.74	0.32	−0.36	1.26**	0.06	0.50**	0.71**	−0.01	1.05**	0.74**
46	−0.85	0.05	0.04	−0.09	0.27	−0.29	0.05	0.47	−0.10**	0.19	0.64**	−0.15+	0.68*	0.21
47	−0.30	0.21	−0.32	−0.45	0.52	0.23	0.12	1.58**	0.09*	0.59**	0.85**	−0.10	1.26*	0.78**
48	0.30	0.17	0.38	−0.08	0.36	0.53	0.62	0.89*	−0.08*	0.28*	0.78**	−0.10	1.06**	0.45+
49	0.44	−0.05	−0.42	0.26	0.30	0.63	−0.54	1.36***	0.09	0.47**	0.85***	0.00	1.14**	0.76**
50	0.64	0.31	−0.05	0.25	0.27	0.56	0.19	1.47***	0.10	0.60**	0.86***	−0.01	1.31***	0.88**
51	0.85	−0.19	−0.13	0.61	0.35	1.19	−0.12	1.57***	0.14*	0.53**	0.98***	0.00	1.45***	0.95**
52	−0.80	0.22	−0.19	−0.36	0.30	−0.39	−0.23	0.44	−0.07	0.28+	0.58*	−0.27**	0.57+	0.19
53	−0.32	−0.06	−0.26	−0.24	0.67	0.37	−0.30	1.20**	0.06	0.52**	0.75**	−0.14	1.08**	0.75*
54	1.10	0.15	0.14	0.78+	0.31	0.96	0.73	1.54**	0.02	0.63**	0.87***	−0.07	1.37**	0.92**
55	0.94	−0.02	−0.18	0.34	0.59	0.81	0.73	1.48**	0.10	0.56**	0.84**	−0.01	1.21**	0.99**
56	−0.44	−0.05	−0.24	−0.20	0.13	0.12	−0.44	0.87+	−0.02	0.39*	0.68*	−0.17	0.89+	0.49
57	0.28	−0.19	−0.24	0.25	0.40	0.44	−0.01	1.55**	0.16+	0.53*	0.94***	0.00	1.36**	0.84*
58	−0.49	−0.02	−0.29	−0.93	0.82	0.03	−0.10	1.08*	0.05	0.39*	0.70*	−0.14	0.87*	0.60+
59	0.80	0.32	0.05	−0.44	0.82	0.92	1.02	1.39*	0.07	0.63**	0.89**	−0.08	1.16*	0.94*
60	−0.68	−0.22	−0.30	−0.46	0.58	−0.25	−0.24	1.66**	0.10+	0.59**	0.93***	−0.01	1.42**	1.00**
61	−0.21	−0.12	0.07	−0.17	0.34	0.43	−0.01	1.46**	0.00	0.51*	0.94***	−0.08	1.36**	0.77*
62	−0.05	0.29	0.08	−0.37	0.55	0.08	0.35	1.15*	0.05	0.56*	0.72**	−0.13	1.02*	0.70*
63	0.17	0.42	0.02	−0.24	0.63	−0.04	0.38	1.32**	0.07	0.63**	0.66**	−0.02	1.10*	0.86*
64	1.34	0.05	0.11	0.51	0.67	1.46*	0.66	1.71**	0.13+	0.79***	1.10**	−0.04	1.36**	1.22**
65	0.32	0.07	0.06	0.26	0.40	0.81	0.01	1.91**	0.18**	0.81**	1.02**	0.02	1.58**	1.34**
66	1.32	−0.08	0.10	0.36	0.97*	1.79**	0.14	2.09***	0.16+	0.82***	1.11***	0.07	1.74***	1.36***
67	0.86	−0.05	0.08	0.25	0.44	1.29+	0.08	1.89***	0.13	0.97***	1.19**	−0.01	1.62**	1.39***
68	0.20	−0.11	−0.30	0.27	0.50	0.79	−0.13	1.63**	0.08	0.69***	0.88**	0.01	1.34**	0.97**
69	−0.84	−0.44	−0.42	0.00	0.07	0.04	−1.03	2.18***	0.25**	0.87***	1.11**	0.12	1.78***	1.44***

(*continued on next page*)

Table 2 (*continued*)

No.[1]	Precipitation (mm/yr)							Reference evapotranspiration (mm/yr)						
	A	W	Sp	Su	Au	Apr–Oct	Oct–Jun	A	W	Sp	Su	Au	Apr–Oct	Oct–Jun
70	−1.59**	−0.61*	−0.59*	−0.29	−0.01	−0.69	−1.45*	1.92**	0.11*	0.68**	0.94**	0.20	1.62**	0.98**

Note: 1 – stations are ordered from west to east, based on increasing longitude coordinate values (the order is the same as in the Fig. 1 and Table 1); "+", "*", "**" and "***" indicate significance at α = 0.1, 0.05, 0.01 and 0.001 level (values without these symbols show lack of statistical significance).

−1.17 mm/yr for the annual CWB decrease, and of −61.96 mm/53 yrs for the index's net decrease (Table 3).

Seasonally, CWB changes show high spatial variability, reflected in dominant/exclusive increases of the humidity deficit in winter, spring and summer, and humidity increase in autumn (Table 3). In the first instance, as it was to be expected, the amplest mean increases of the climatic water deficit occurred in summer and ranged from −1.54 mm/yr/−81.45 mm/53 yrs (Southern Carpathians) to −0.60 mm/yr/−31.62 mm/53 yrs (Subcarpathians) (Table 3). In terms of spatial macrounits, it is however surprising that the Carpathian region had the most apparent drier changes (−1.12 mm/yr/−59.22 mm/53 yrs), instead of the Extra-Carpathian region, which is in return the hotspot of mean CWB decreases in winter and spring (Table 3). Overall, the humidity deficit conditions in Romania in the warmest period of the year increased by −0.93 mm/yr and − 49.04 mm/53 yrs (Table 3).

In the second case, in autumn, the annual climatic humidity increase ranges from 0.08 mm/yr (Danube Delta) to 1.03 mm/yr (Western Carpathians), and is equivalent to an interval of net changes in humidity conditions between 4.40 and 54.36 mm/53 yrs (Table 3). Out of the three major regions, the Carpathians became the wettest in this transitional season (0.81 mm/yr/42.75 mm/53 yrs) (Table 3). At the same time, the climatic water excedent increased, on average, by 0.69 mm/yr/36.35 mm/53 yrs across the entire national territory (Table 3).

While the growing seasons of the two agricultural crops were marked by significant water deficit amplification across the country, the highest increases were noticed in the wheat growing season, when annual/net CWB changes ranged from −2.16 mm/yr/−114.48 mm/53 yrs (Mehedinti Hills) to −0.43 mm/yr/−22.70 mm/53 yrs (Crisanei Hills) (Table 3). The mean increase in dryness conditions reached a peak in the Extra-Carpathian region (−1.23 mm/yr/−65.28 mm/53 yrs) (Table 3). In this period, Romania's entire territory experienced a mean annual humidity deficit increase rate of −1.10 mm, which is equivalent to a total change of −58.33 mm over the entire period 1961–2013 (Table 3).

3.4. Climatic water balance variability in relation to large-scale atmospheric circulation

The methodology used in this respect enabled us to analyse the relation between the analysed elements not only in terms of correlation strength resulting from Spearman test results, but also in terms of the quantitative difference of CWB based on the phase of each teleconnection. For instance, between the years with high and low NAO and CWB values, a negative correlation of −0.35 was identified annually for the Carpathian and Extra-Carpathian regions (Table 4). This denotes higher CWB values during low NAO years and vice versa in these extensive regions of the country. Additionally, by means of a composite analysis, we found that the difference between high and low NAO years causes, for instance, a CWB variability of ± 130.5 mm in the Carpathian area, on the same analysed time scale (Table 5).

Overall, most teleconnections indices display negative correlations with CWB in Romania (Table 4). In other terms, positive phases of the teleconnections analysed here are associated with negative CWB values, i.e. with a climatic water deficit increase. In this respect, it can indirectly be stated that the amplification of dryness trends identified on all time scales (except for autumn) is generally associated with an increasing cases of positive phases for the analysed teleconnection indices. Only the Scandinavian Pattern disrupts this general rule, as positive SP is correlated with positive CWB values (water excedent increase) in most cases (Table 4).

Annually, AO is the only driver having a generalized impact on CWB in the three major regions (considering the Spearmann correlation coefficients, which are statistically significant in all 3 cases), and, therefore, across the country (Table 4). Moreover, AO imposes the strongest variability on this temporal scale, which reaches a ± 140.3 mm peak in the Carpathians region when the values of this teleconnection index reach the extremes (Table 5). Also, while the second most important teleconnection annually is NAO, its induced variability upon CWB in Romania is lower and felt only in the Carpathian (± 130.5 mm) and Extra-Carpathian (± 112.5 mm) regions (Table 5). Apart from this, SP, EA and AMO indicate a clear signal annually, which is however less intense (less than ± 100 mm) and restricted to the Intra-Carpathians region (Table 5).

In winter and spring, a high CWB response can be noticed especially in AO, NAO and EAWR dynamics, across the country (Tables 4, 5). In spring, regardless of the region, the variability imposed by AO (more than ± 65 mm in CWB variability) or NAO (more than ± 45 mm) is the highest compared to the other seasons (Table 5). EAWR has a discernible impact that is higher especially during winter in Romania (more than ± 30 mm), except for spring in the Carpathians region (Table 5).

The other two seasons also show interesting connections between atmospheric circulation and CWB dynamics. During summer, the CWB is driven by certain mechanisms related to the specifics of ocean-atmosphere couple in North Atlantic (EA and AMO), as each of the two mentioned teleconnections induces a CWB variability that is generally higher than ± 50 mm, negatively correlated and generalized for all the regions (Tables 4, 5). In autumn, a notable influence of AO can be noticed in CWB dynamics (more than ± 45 mm), which is associated to the proximity to the cold season. We must however also underline the interesting significant differences in the field of CWB between intense western and eastern winds in the equatorial stratosphere, as reflected by QBO (higher than ± 30 mm) (Table 5).

The maize growing season seem to be modelled only by AMO (Table 4), with an imposed variability on CWB which exceeds ± 80 mm in all three regions (statistically significant only in Intra-Carpathian and Extra-Carpathian regions) (Table 5). At the same time, the wheat growing season is generally influenced by a couple of teleconnections (AO, NAO, EAWR), if considering the entire country, as well as by the SP index, if only considering the Intra-Carpathian and Extra-Carpathian regions (Tables 4, 5).

4. Discussions

4.1. Influence of atmospheric dynamics on climatic water balance variability

The high overall impact of AO on CWB in Romania is not a surprise since AO is known to be an important contributor to climate variability, especially in winter, in all Eurasia (Yeo et al., 2017). Our study suggests that an intense zonal flow associated with positive AO induces a general

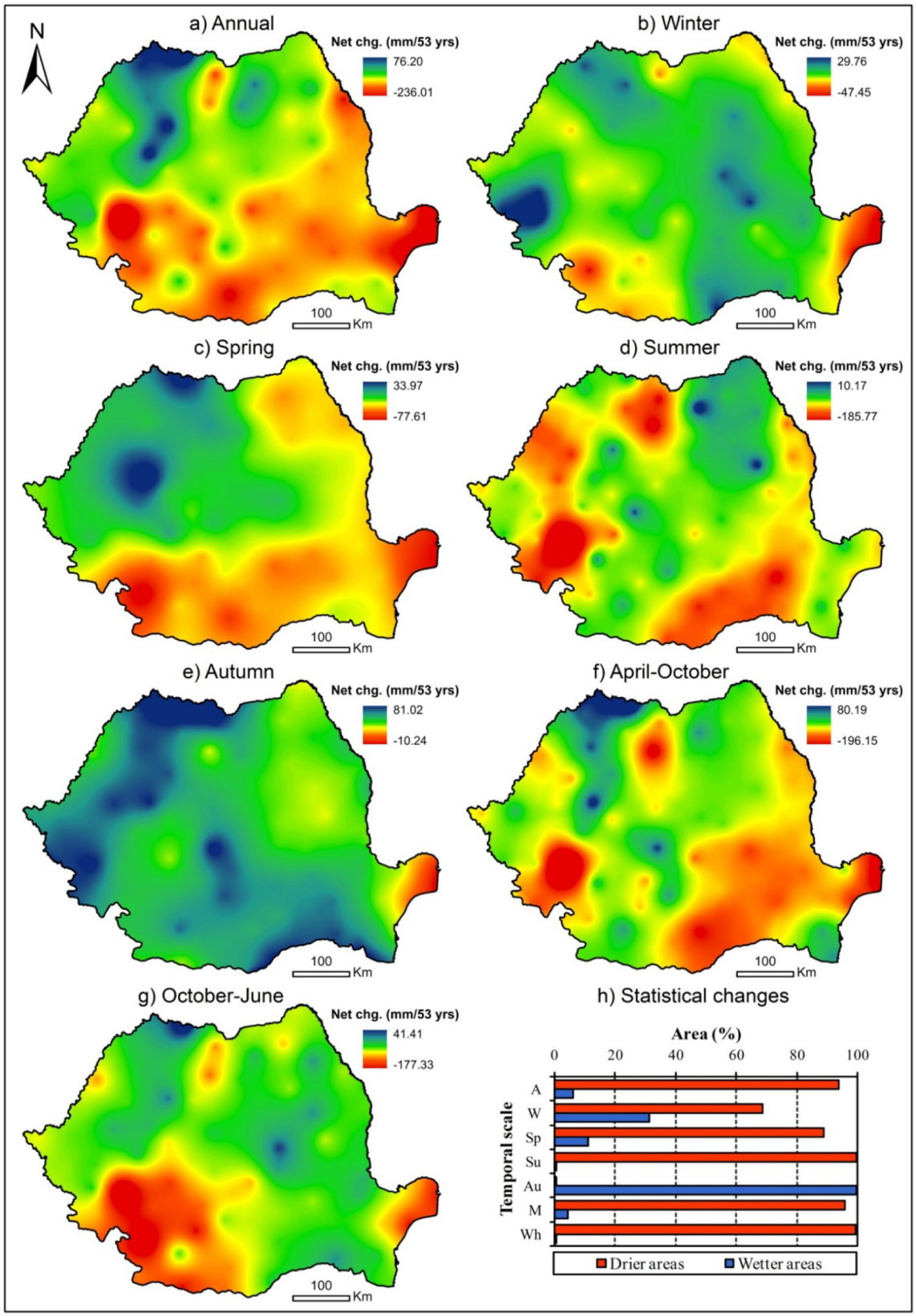

Fig. 5. Climatic water balance net changes on the seven temporal scales, in the 1961–2013 period. Note: the statistical data on the bottom right-hand side (*A* annual, *W* winter, *Sp* spring, *Su* summer, *Au* autumn, *M* maize growing season, *Wh* wheat growing season) were extracted by setting two classes on the rasters with net changes, i.e. < 0 mm/53 yrs (drier areas) and > 0 mm/53 yrs (wetter areas).

Table 3
Mean spatial values of annual (mm/yr) and net (mm/53 yrs) changes in the climatic water balance (CWB) in the period 1961–2013, on the seven analysed temporal scales (*A* annual, *W* winter, *Sp* spring, *Su* summer, *Au* autumn, *Apr–Oct* maize growing season, *Oct–Jun* wheat growing season).

No.	Spatial units	Annual CWB changes (mm/yr)							Net CWB changes (mm/53 yrs)						
		A	W	Sp	Su	Au	Apr–Oct	Oct–Jun	A	W	Sp	Su	Au	Apr–Oct	Oct–Jun
1	Eastern Carpathians	−0.69	−0.04	−0.13	−0.93	0.82	−0.47	−0.56	−36.61	−1.97	−7.10	−49.38	43.64	−24.72	−29.70
2	Curvature Carpathians	−1.83	0.03	−0.36	−0.87	0.58	−1.15	−0.88	−96.79	1.52	−19.29	−45.97	30.90	−60.96	−46.44
3	Southern Carpathians	−1.77	−0.11	−0.07	−1.54	0.67	−1.03	−1.76	−93.94	−5.60	−3.94	−81.45	35.76	−54.41	−93.13
4	Banatului Carpathians	−0.61	0.26	−0.32	−1.27	1.02	−1.01	−1.13	−32.55	13.52	−17.11	−67.53	53.86	−53.75	−60.10
5	Western Carpathians	−0.14	−0.28	0.42	−1.02	1.03	−0.24	−0.63	−7.44	−14.86	22.21	−54.19	54.36	−12.93	−33.58
6	Transylvanian Plateau	−0.75	−0.02	−0.11	−0.92	0.60	−0.78	−0.99	−39.81	−0.91	−6.05	−48.77	32.06	−41.25	−52.41
7	Crisanei Hills	−0.17	0.01	−0.01	−1.24	1.01	−0.27	−0.43	−9.25	0.75	−0.37	−65.58	53.64	−14.24	−22.70
8	Banatului Hills	−0.69	0.31	−0.27	−0.80	0.87	−0.78	−0.81	−36.61	16.55	−14.50	−42.40	46.22	−41.35	−42.80
9	Subcarpathians	−1.30	0.02	−0.62	−0.60	0.53	−0.68	−1.18	−69.02	0.80	−32.68	−31.62	27.84	−36.14	−62.66
10	Mehedinti Hills	−1.95	−0.42	−1.14	−0.97	0.51	−0.94	−2.16	−103.35	−22.26	−74.73	−51.41	27.03	−49.82	−114.48
11	Getic Plateau	−1.58	−0.41	−1.04	−0.87	0.77	−0.72	−2.10	−83.75	−21.83	−55.26	−46.34	40.55	−38.17	−111.10
12	Moldavian Plateau	−1.23	−0.23	−0.70	−0.73	0.49	−0.74	−0.95	−65.33	−12.14	−37.21	−38.73	25.79	−39.10	−50.18
13	Western Plain	−0.59	−0.03	−0.22	−0.86	0.78	−0.48	−1.08	−31.18	−1.50	−11.88	−45.69	41.13	−25.19	−57.42
14	Romanian Plain	−1.38	−0.08	−0.82	−0.98	0.79	−0.87	−1.02	−73.36	−4.30	−43.31	−52.00	42.08	−46.19	−54.09
15	Dobrogea Plateau	−1.31	−0.27	−0.73	−0.78	0.57	−0.33	−1.04	−69.60	−14.19	−38.74	−41.27	30.04	−17.67	−54.90
16	Danube Delta	−2.68	−0.67	−1.19	−0.95	0.08	−1.48	−2.01	−142.25	−35.33	−63.33	−50.30	4.40	−78.41	−106.63
17	Carpathians region	−1.01	−0.04	−0.10	−1.12	0.81	−0.72	−0.96	−53.27	−2.11	−5.52	−59.22	42.75	−38.00	−50.63
18	Intra-Carpathians region	−0.62	0.01	−0.15	−0.94	0.73	−0.61	−0.93	−32.64	0.28	−7.80	−49.56	38.91	−32.30	−49.48
19	Extra-Carpathians region	−1.46	−0.19	−0.81	−0.84	0.61	−0.79	−1.23	−77.43	−9.93	−42.75	−44.29	32.48	−41.92	−65.28
20	Romania	−1.17	−0.11	−0.49	−0.93	0.69	−0.73	−1.10	−61.96	−5.84	−26.21	−49.04	36.35	−38.90	−58.33

Note: the mean spatial values were obtained by averaging annual rates and total changes over the 53 years recorded by the weather stations located in the analysed spatial units.

climatic water deficit in Romania since AO is known to have an increasing trend during the last decades (Fyfe et al., 1999). The weaker response of AO in the Carpathians region, considering the Spearman correlation results compared to the other two regions delimited in Romania (Table 4), is a result of the fact that most of the region's weather stations are located in valleys or mountain depressions, and are thus sheltered from the atmospheric circulation. On mountain tops, the impact of AO is normally expected to be greater. In fact, in terms of composite analysis, the impact of AO is generally greater in the mountain region compared to the other two regions of the country (Table 5).

A similar relation appears for NAO due to the fact that this teleconnection can be seen as a regional equivalent of AO for the Euro-Atlantic region (Scaife et al., 2014). However, the relation is less intense and restricted to winter and spring, since the NAO signal strength diminishes during summer inside the European continent, as shown by other studies (Casanueva et al., 2014). Also, NAO presents a similar increasing trend as AO (Krichak et al., 2002), explaining at least partially the observed increase in water deficit observed in Romania.

EA represents a teleconnection for which the centres of action specific to NAO are shifted to the south in the Atlantic (Barnston and Livezey, 1987), and are also considered to have an important role in the structure of NAO (Moore and Renfrew, 2012). Under these conditions, the axis of circulation is shifting from West to East during NAO+ to

Table 4
Spearmann corelation coefficients (1961–2013) in the three major Romanian regions between climatic water balance and different teleconnection indices (*AO* Arctic Oscillation, *NAO* North Atlantic Oscillation, *SP* Scandinavian Pattern, *EA* East Atlantic, *EAWR* East Atlantic-Western Russia, *AMO* Atlantic Multi-Decadal Oscillation, *QBO* Quasi-Biennal Oscillation), for the seven temporal levels (*A* annual, *W* winter, *Sp* spring, *Su* summer, *Au* autumn, *Apr–Oct* maize growing season, *Oct–Jun* wheat growing season).

No.	Spatial units	Temporal scale	AO	NAO	SP	EA	EAWR	AMO	QBO
1.	Carpathians region	A	**−0.41**	**−0.35**	+0.21	−0.24	−0.19	−0.22	−0.02
		W	**−0.48**	**−0.34**	−0.01	+0.21	**−0.41**	+0.23	−0.02
		Sp	**−0.51**	**−0.47**	−0.11	−0.09	**−0.33**	−0.05	−0.09
		Su	+0.11	+0.06	**+0.30**	−0.19	+0.12	**−0.39**	+0.09
		Au	**−0.29**	−0.15	−0.04	**−0.36**	−0.21	+0.04	−0.12
		Apr–Oct	−0.21	−0.12	+0.18	−0.15	−0.01	**−0.33**	+0.02
		Oct–Jun	**−0.46**	**−0.30**	+0.18	−0.22	**−0.39**	−0.14	−0.08
2.	Intra-Carpathians region	A	**−0.42**	−0.22	**+0.31**	**−0.34**	−0.14	**−0.34**	+0.08
		W	**−0.61**	**−0.41**	**+0.35**	−0.17	**−0.59**	+0.16	−0.07
		Sp	**−0.54**	**−0.43**	+0.03	**−0.29**	−0.21	**−0.26**	−0.08
		Su	+0.18	**+0.27**	**+0.27**	−0.22	+0.14	**−0.40**	+0.18
		Au	**−0.34**	−0.18	+0.16	−0.26	−0.23	+0.07	−0.16
		Apr–Oct	−0.20	+0.02	+0.17	−0.22	−0.05	**−0.39**	+0.16
		Oct–Jun	**−0.56**	**−0.34**	**+0.32**	−0.20	**−0.42**	−0.21	−0.12
3.	Extra-Carpathians region	A	**−0.50**	**−0.35**	+0.18	−0.16	−0.24	−0.19	−0.06
		W	**−0.57**	**−0.37**	+0.05	−0.07	**−0.37**	+0.23	−0.07
		Sp	**−0.50**	**−0.42**	−0.03	0.00	**−0.30**	−0.05	−0.09
		Su	+0.02	−0.08	+0.25	−0.17	+0.09	**−0.37**	+0.06
		Au	**−0.34**	−0.16	−0.03	**−0.31**	−0.13	+0.02	−0.14
		Apr–Oct	−0.26	−0.15	+0.11	−0.13	0.00	**−0.31**	+0.00
		Oct–Jun	**−0.54**	**−0.28**	+0.24	0.00	−0.32	−0.14	−0.13

Note: the values in bold are statistically significant at 0.05 level of significance.

Table 5
Climatic water balance index variability (1961–2013) in the three major Romanian regions between upper and lower thirds of the eight teleconnection indices (*AO* Arctic Oscillation, *NAO* North Atlantic Oscillation, *SP* Scandinavian Pattern, *EA* East Atlantic, *EAWR* East Atlantic-Western Russia, *AMO* Atlantic Multi-Decadal Oscillation, *QBO* Quasi-Biennal Oscillation), for the seven temporal levels (*A* annual, *W* winter, *Sp* spring, *Su* summer, *Au* autumn, *Apr–Oct* maize growing season, *Oct–Jun* wheat growing season).

No.	Spatial units	Temporal scale	AO	NAO	SP	EA	EAWR	AMO	QBO
1.	Carpathians region	A	**−140.3**	**−130.5**	+51.1	−78.7	−75.7	−75.9	−8.4
		W	**−52.3**	**−37.5**	−2.0	−9.3	**−36.5**	+11.3	−7.8
		Sp	**−71.2**	**−58.6**	−17.3	−18.6	**−39.8**	−9.7	−7.3
		Su	+24.3	+19.1	+53.1	**−51.5**	+32.4	**−72.3**	+22.3
		Au	**−50.9**	−24.9	−12.7	**−47.3**	−18.6	+1.1	**−36.8**
		Apr–Oct	−47.8	−40.7	+37.9	−58.2	+20.8	−94.1	+0.8
		Oct–Jun	**−90.6**	**−65.6**	+50.7	−50.1	**−76.5**	−20.5	−24.3
2.	Intra-Carpathians region	A	**−116.4**	−55.7	**+59.9**	**−95.8**	−41.0	**−84.3**	+10.7
		W	**−54.9**	**−42.6**	**+31.1**	−9.5	**−56.1**	+8.9	−12.6
		Sp	**−66.6**	**−49.0**	−3.45	**−45.5**	−19.8	**−31.2**	−3.2
		Su	+31.8	**+46.4**	+39.2	**−51.5**	+32.4	**−56.5**	+28.8
		Au	**−49.3**	−14.3	+16.9	−28.8	−11.1	+2.6	**−33.5**
		Apr–Oct	−21.1	+12.8	+20.9	−56.9	−3.8	**−80.4**	+19.9
		Oct–Jun	**−99.9**	**−57.5**	**+68.2**	−52.7	**−71.6**	−43.2	−21.6
3.	Extra-Carpathians region	A	**−133.0**	**−112.5**	+34.7	−67.8	−68.0	−73.0	−21.4
		W	**−52.2**	**−36.3**	+0.3	−0.6	**−32.4**	+9.4	−5.7
		Sp	**−68.1**	**−51.8**	−8.1	**−45.5**	−19.8	−9.7	−7.3
		Su	+4.4	−3.02	+41.3	**−46.8**	+31.6	**−67.4**	+10.6
		Au	**−46.2**	−26.3	−8.5	−30.8	−16.4	0.0	**−31.9**
		Apr–Oct	−62.9	−40.2	+14.7	−46.6	+18.5	**−93.0**	−12.2
		Oct–Jun	**−98.6**	−56.8	**+61.7**	−0.9	**−58.0**	−24.7	**−31.3**

Note: the values in bold are statistically significant at 0.05 level of significance.

South-West to North-East during EA+. Positive EA is related to troughs development in the North Atlantic while the European continent is dominated by positive SLP anomalies that determine positive anomalies in the field of temperature in south-eastern Europe (Knežević et al., 2014) and consequently negative anomalies in precipitation in Romania's region in the warm seasons (NOAA, 2017a). These conditions are leading both to climatic water deficit in Romania, which explains the statistically significant negative correlation between EA and CWB especially in summer in our study. Inversely, as shown by Knežević et al. (2014), negative EA is related to deep troughs development in central Europe which explains the same negative correlation with CWB in Romania in summer.

Significant correlations between AMO and CWB prevail in Romania as well, which can be related to the fact that positive AMO was found to increase extratropical cyclonicity in summer (Knight et al., 2006), with a peak identified in the eastern part of the North Atlantic extended towards Europe (Dima and Lohmann, 2007). However, as our results show, in summer correlations are not statistically significant in Romania, due to the fact that the Atlantic cyclones formed under the influence of warm oceanic waters generate higher amounts of precipitation in Western Europe (Sutton and Hodson, 2005), but are progressively deprived of precipitation when they reach Eastern/Southeastern Europe. At the same time, in Romania, evapotranspiration increases due to more intense wind speeds associated with cyclonic activity, which leads to a higher water deficit associated to AMO+.

The effect of QBO on CWB in Romania, generally restricted to autumn in the composite analysis, could be determined by this season's lower sensitivity to the hemispherical teleconnection action that makes perceptible the possible influence of QBO. Considering that the negative phase of QBO is related to the weakening of the polar vortex and an increase in blocking frequency in Europe (Thompson et al., 2002), the observed negative correlation in our study indicated by the composite analysis in autumn for Romania is logical and connected to the increase in humidity conditions in this season across the country. This possible mechanism is also confirmed by our results on the Scandinavian Pattern, a teleconnection that reflects the anticyclonic blocking activity centred in Scandinavia (NOAA, 2017a), which in return causes humidity conditions at low latitudes, such as central south-eastern Europe, where Romania is located (this is reflected in the negative correlations generally identified in our study, which are however not statistically significant). In contrast, the positively correlated pattern with the CWB index in Romania, especially for the wheat growing season, but also for the summer season (Tables 4, 5), is related to the role of blocking development for the occurrence of precipitation in Romania (Rimbu et al., 2016). This reasoning is consistent with our results on dryness trends (almost exclusively negative CWB trends) in these two periods, since decreasing trends in SP have been observed during the last decades (Rodriguez-Puebla et al., 1998).

Another teleconnection analysed in this study is EAWR, which has a strong influence on climate conditions especially in the central and southern parts of Europe (Ionita, 2014), and is related to a negative correlation in the fields of temperature and precipitation (NOAA, 2017a). EAWR is more active in winter and display a positive trend (Krichak and Alpert, 2005), our results confirming this general rule. The negative correlation identified between EAWR and CWB in Romania is explained mainly by the similar correlation found between EAWR and precipitation in Europe in winter and in the first half of spring (Ionita, 2014).

4.2. Climatic water balance dynamics and its implications on anthropic and ecological systems

For Europe, our results are consistent with the general pattern of dryness trends in the continent's southeastern region, identified at least partially in certain global (Greve et al., 2014) or regional (Cheval et al., 2017) studies. While these studies identified a clear increase in the climatic water deficit (in certain significant areas of this continental region that also encompasses Romania) based on several aridity indices, an overall comparison of our results to these studies can be made considering that dryness changes in southeastern Europe were analysed exclusively/including based on precipitation and evapotranspiration. However, considering the methodology for computing aridity indices (which include the two parameters as a ratio, instead of difference as with the CWB) and the lack of annual/net changes investigation of aridity indices, a concrete comparison of our results to these analyses is not possible.

Moreover, our findings are overall in agreement with national studies, which have directly or indirectly signalled the transition, in recent

decades, of large areas of the country towards drier conditions, based either on the analysis of aridity indices in the Extra-Carpathian region (Croitoru et al., 2013c) or on separate analyses of precipitation (Dumitrescu et al., 2015) and evapotranspiration (Croitoru et al., 2013a) dynamics across Romania's territory. However, in this case too, a direct comparison of our results (e.g. on annual CWB decrease rates) to these studies is not possible, considering that the CWB index has not been analysed before in terms of trends or overall dynamics, neither nationally, nor regionally. This does not apply for our results on separate P (some statistically significant increasing/decreasing trends in the northwest/southeast annually, and seasonal trends that are generally not statistically significant, except for autumn, with several positive statistically significant trends) and ET_o (mostly positive annual and seasonal trends, generally statistically significant, except for autumn, with trends that are dominantly negative and partially statistically significant) trends, which are in strong agreement with previous studies (Croitoru et al., 2013a; Marin et al., 2014; Dumitrescu et al., 2015).

Regarding the results of CWB changes, it must be noted that the general dryness trend recorded in the past half-century, identified in this paper on all time scales (except for autumn) and for most of the national territory, must be interpreted cautiously considering that negative CWB trends generally have a low statistical significance. We inferred that dryness trends are general for Romania considering the predominant extent of the negative CWB trends and the magnitude of the changes (generally high water deficit amplification slopes), but it must be noted that the statistical significance of these trends is currently limited. The exceptions to this overall state of affairs consist of the regional hotspots (especially the country's southwest and southeast), where statistically significant trends indicate clear climatic dryness over the past decades. However, we believe an anticipation of clear dryness trends can be brought into discussion, which could become statistically significant on a large scale in the near future, if CWB trends continue to decrease at the same intensity.

Even with the current CWB dynamics, we believe the general dryness pattern already identified on Romania's territory can account for the occurrence and amplification of a wide range of negative consequences on anthropic and natural systems. These possible negative effects are multidimensional and include, for instance, implications on perturbations of agricultural systems, water resources, forest vegetation, ecological state of lands and biodiversity.

In the first case, it was already found that maize crop yields decreased (after 1990) on average by almost 1 t/ha/yr in the southeast for a 100 mm rise in the climatic water deficit (Prăvălie et al., 2014a), or even by ~1.7 t/ha/yr in the southwest, for the same CWB variation (Prăvălie et al., 2016b). In terms of water resources, an overall decrease in river discharge was noticed nationally after 1961, especially during the summer season, which can be explained by the season's more intense evaporation processes (Birsan et al., 2014), and consequently by a higher humidity deficit, keeping in mind that precipitation remained relatively stable across the country in this time of the year (Dumitrescu et al., 2015). Also, certain studies conducted in Extra-Carpathian sectors highlighted the vulnerability of groundwater level to oscillations in precipitation and evapotranspiration, i.e. to the disruption of the CWB (Cocos et al., 2012; Minea and Croitoru, 2017).

The degradation of wetlands is another major threat of a drier climate, especially in the Extra-Carpathian area, where most such ecological systems are found. It appears that the Danube Delta, the most compact reed area worldwide, but also the most extensive in the European Union and the largest continuous marshland in Europe (PRDD, 2014; Giosan et al., 2014), is already being affected by a series of negative effects (Prăvălie et al., 2016a) partly due to the amplification of the humidity deficit, which has had a much more aggressive rate in this region (Fig. 3). The importance of such climatic perturbations is all the more significant considering that the Danube Delta is a global biodiversity hotspot – it brings together 5000 fauna species and about 2000 species of plants (Giosan et al., 2014).

The degradation of forest vegetation is another impact vector for the changing humidity conditions across the country. Instances of forest dieback were already signalled in certain areas in southwestern Romania, as a result of high thermal stress (and of an intense evapotranspiration regime), coupled with low precipitation amounts (Prăvălie et al., 2014b). Recent indirect reports on CWB changes (higher evapotranspiration) were made in the Carpathian area (Nistor et al., 2016) as well, which could entail possible negative effects on valuable ecosystem services (provisioning, regulating, supporting and cultural services) provided by forests, especially in this region where forest ecosystems cover by far the most extensive areas in the country.

The ecological state of lands can also be seriously threatened in an environment with less water availability (Prăvălie et al., 2017b). Recently, it was found that extensive land areas had become more sensitive to degradation, especially the Extra-Carpathians region, against the background of a significant multiannual humidity deficit that also determined the presence and expansion of dry sub-humid and semi-arid areas in these lowlands of the country (Prăvălie et al., 2017a).

Threats to biodiversity are also an issue Romania could face underdrier climatic conditions. It seems this ecological problem will escalate significantly. For instance, it is expected that, over the following decades, certain taxonomic groups of animals, especially amphibians (particularly sensitive to humidity variations) will be affected by notable range contractions as moisture availability decreases across the country (Popescu et al., 2013). This overall future decrease was also foreseen by climatic studies on Southeastern Europe (Gao and Giorgi, 2008; Cheval et al., 2017). Nonetheless, it is estimated that the Carpathian region will act as a major climate refugia for many animal species (Popescu et al., 2013), as it will be affected to a lesser extent by future climate change compared to the Intra-Carpathian and Extra-Carpathian regions of the country.

5. Conclusions

This paper analyses a climatic issue that has yet to be explored in Romania, i.e. climatic water balance dynamics in the past half-century, in relation to P and ET_otrends, which are responsible for CWB pattern changes. The statistical analyses conducted by means of the well-established methods Mann-Kendall test and *Sen's slope*, which were applied to climatic data recorded at 70 weather stations distributed uniformly countrywide, showed that Romania has experienced drier conditions in the 1961–2013 period annually, seasonally (except for autumn) and in the maize and wheat growing seasons. Overall, the negative CWB trends on the analysed time scales (of up to −2 mm/yr in most cases) have turned extensive regions into drier areas, which in most cases covered over 90% of the national territory. Our investigation on the influence of atmospheric circulation on CWB variability also showed that the general pattern of drier trends is especially linked to the positive phases of the Arctic Oscillation and North Atlantic Oscillation, and, in part, to those of several other teleconnection indices that affect the European territory.

Our results showed that the main hotspots of climatic water deficit amplification are the southwest and southeast, as these regions experienced the amplest annual (statistically significant in most cases) and net CWB decreases. Thus, we can conclude that, statistically, drier trends are clear in Romania only regionally. We must therefore draw attention to the trends' significance (which is relatively limited nationally at this time), even though negative CWB trends were observed countrywide, generally with a high magnitude that was assessed in terms of annual and net changes. At the same time, we believe that in the near future a clear presence of dry conditions is likely to be noticed throughout Romania, if the negative CWB changes continue to occur with the same intensity. The most important clue that strengthens this argument is ET_o dynamics, which has already experienced strong statistically significant increasing trends (at high and very high α thresholds), generally at national level and with clearly higher slopes

compared to P. Given these conditions, in the coming years, it is very likely that these dynamics, which will intensify against the background of a warmer world, will sufficiently counterbalance the uncertainty of P and transform vast territories of Romania into clearly drier areas.

Even with the current CWB dynamics, the overall amplification of the water deficit in Romania can be responsible for triggering and/or amplifying various anthropic (agricultural) and ecological (lower water resources, degradation of forest vegetation, lands' ecological state, and biodiversity) consequences, especially in the country's Intra-Carpathian and Extra-Carpathian regions, where CWB decreases were the most intense in the past half-century. Therefore, we recommend this hypothesis be analysed concretely in future agro-climatic, hydro-climatic and eco-climatic studies, in an interdisciplinary manner and on a national scale. Such studies are necessary to help anthropic and ecological systems adapt to a drier future, which seems to be imminent, for Romania as well, in the 21st century.

Acknowledgements

The authors would like to thank the anonymous reviewers for their highly constructive comments and suggestions that helped improve this paper. All authors contributed equally to this article.

References

Allen, R.G., Pereira, L.S., Raes, D., Smith, M., 1998. Crop evapotranspiration: guidelines for computing crop water requirements. In: FAO Irrigation and Drainage Paper 56, Rome, Italy.
Apostol, L., Sfîcă, L., 2013. Thermal differentiations induced by the Carpathian Mountains on the Romanian territory. Carpath. J. Earth Environ. Sci. 8, 215–221.
Ávila, A., Justino, F., Wilson, A., Bromwich, D., Amorim, M., 2016. Recent precipitation trends, flash floods and landslides in southern Brazil. Environ. Res. Lett. https://doi.org/10.1088/1748-9326/11/11/114029.
Bandoc, G., Prăvălie, R., 2015. Climatic water balance dynamics over the last five decades in Romania's most arid region, Dobrogea. J. Geogr. Sci. 25, 1307–1327.
Barnston, A.G., Livezey, R.E., 1987. Classification, seasonality and persistence of low-frequency atmospheric circulation patterns. Mon. Weather Rev. 115, 1083–1126.
Barriopedro, D., García-Herrera, R., Huth, R., 2008. Solar modulation of Northern Hemisphere winter blocking. J. Geophys. Res. 113. https://doi.org/10.1029/2008JD009789.
Bastia, F., Equeenuddin, S.M., 2016. Spatio-temporal variation of water flow and sediment discharge in the Mahanadi River, India. Glob. Planet. Chang. 144, 51–66.
Birsan, M.V., Dumitrescu, A., 2014. ROCADA: Romanian Daily Gridded Climatic Dataset (1961–2013) V1.0. National Meteorological Administration, Bucharest, Romania. https://doi.org/10.1594/PANGAEA.833627.
Birsan, M.V., Zaharia, L., Chendes, V., Branescu, E., 2014. Seasonal trends in Romanian streamflow. Hydrol. Process. 28, 4496–4505.
Bonan, G.B., 2008. Forests and climate change: Forcings, feedbacks, and the climate benefits of forests. Science 320, 1444–1449.
Busuioc, A., Caian, M., Cheval, S., Bojariu, R., Boroneanţ, C., Baciu, M., Dumitrescu, A., 2010. Climate Variability and Change in Romania. Pro Universitaria Publishing, Bucharest, Romania (in Romanian).
Byrne, M.P., O'Gorman, P.A., 2015. The response of precipitation minus evapotranspiration to climate warming: why the "wet-get-wetter, dry-get-drier" scaling does not hold over land. J. Clim. 28, 8078–8092.
Casanueva, A., Rodríguez-Puebla, C., Frías, M.D., González-Reviriego, N., 2014. Variability of extreme precipitation over Europe and its relationships with teleconnection patterns. Hydrol. Earth Syst. Sci. 18, 709–725.
CDO, 2015. Climate Data Operators. Max Planck Institute for Meteorology. http://www.mpimet.mpg.de/cdo.
Cheval, S., Birsan, M.V., Dumitrescu, A., 2014. Climate variability in the Carpathian Mountains Region over 1961–2010. Glob. Planet. Chang. 118, 85–96.
Cheval, S., Dumitrescu, A., Birsan, M.V., 2017. Variability of the aridity in the South-Eastern Europe over 1961–2050. Catena 151, 74–86.
CLC, 2012. CORINE Land Cover Raster Data. European Environment Agency. www.eea.europa.eu.
Cocos, A., Cocos, O., Sarbu, I., 2012. Coping with water scarcity: the case of the Calnistea catchment (Romania). Environ. Earth Sci. 67, 641–652.
Colantoni, A., Ferrara, C., Perini, L., Salvati, L., 2015. Assessing trends in climate aridity and vulnerability to soil degradation in Italy. Ecol. Indic. 48, 599–604.
Crimmins, S.M., Dobrowski, S.Z., Greenberg, J.A., Abatzoglou, J.T., Mynsberge, A.R., 2011. Changes in climatic water balance drive downhill shifts in plant species' optimum elevations. Science 331, 324–327.
Croitoru, A.E., Piticar, A., Dragotă, C.S., Burada, D.C., 2013a. Recent changes in reference evapotranspiration in Romania. Glob. Planet. Chang. 111, 127–137.
Croitoru, A.E., Chiotoroiu, B.C., Todorova, V.I., Torica, V., 2013b. Changes in precipitation extremes on the Black Sea Western Coast. Glob. Planet. Chang. 102, 10–19.
Croitoru, A.E., Piticar, A., Imbroane, A.M., Burada, D.C., 2013c. Spatiotemporal distribution of aridity indices based on temperature and precipitation in the extra-Carpathian regions of Romania. Theor. Appl. Climatol. 112, 597–607.
Croitoru, A.E., Piticar, A., Ciupertea, A.F., Roşca, C.F., 2016a. Changes in heat waves indices in Romania over the period 1961–2015. Glob. Planet. Chang. 146, 109–121.
Croitoru, A.E., Piticar, A., Burada, D.C., 2016b. Changes in precipitation extremes in Romania. Quat. Int. 415, 325–335.
Demaria, E.M.C., Goodrich, D., Keefer, T., 2017. Frequency analysis of extreme sub-daily precipitation under stationary and non-stationary conditions across two contrasting hydroclimatic environments. Hydrol. Earth Syst. Sci. Discuss. https://doi.org/10.5194/hess-2017-247.
Diffenbaugh, N.S., Field, C.B., 2013. Changes in ecologically critical terrestrial climate conditions. Science 341, 486–492.
Dima, M., Lohmann, G., 2007. A hemispheric mechanism for the Atlantic Multidecadal Oscillation. J. Clim. 20, 2706–2719.
Dobesch, H., Dumolard, P., Dyras, I., 2007. Spatial interpolation for climate data. In: The Use of GIS in Climatology and Meterology. 320 Wiley-ISTE, London.
Dumitrescu, A., Birsan, M.V., 2015. ROCADA: a gridded daily climatic dataset over Romania (1961–2013) for nine meteorological variables. Nat. Hazards 78, 1045–1063.
Dumitrescu, A., Bojariu, R., Bîrsan, M.V., Marin, L., Manea, A., 2015. Recent climatic changes in Romania from observational data (1961–2013). Theor. Appl. Climatol. 122, 111–119.
Enfield, D.B., Mestas-Nunez, A.M., Trimble, P.J., 2001. The Atlantic multidecadal oscillation and it's relation to rainfall and river flows in the continental U.S. Geophys. Res. Lett. 28, 2077–2080.
ESRI, 2012. ArcGIS Desktop: Release 10.1, Redlands, CA. Environmental Systems Research Institute, United States.
Fan, Z.X., Thomas, A., 2013. Spatiotemporal variability of reference evaporation and its contributing climatic factors in Yunnan Province, SW China, 1961–2004. Clim. Chang. 116, 309–325.
Fan, J., Wu, L., Zhang, F., Xiang, Y., Zheng, J., 2016. Climate change effects on reference crop evapotranspiration across different climatic zones of China during 1956–2015. J. Hydrol. 542, 923–937.
Fawcett, A.A., Iyer, G.C., Clarke, L.E., Edmonds, J.A., Hultman, N.E., McJeon, H.C., Rogelj, J., Schuler, R., et al., 2015. Can Paris pledges avert severe climate change? Science 350, 1168–1169.
Feng, S., Fu, Q., 2013. Expansion of global drylands under a warming climate. Atmos. Chem. Phys. 13, 10081–10094.
Feng, Y., Cui, N., Zhao, L., Gong, D., Zhang, K., 2017. Spatiotemporal variation of reference evapotranspiration during 1954–2013 in Southwest China. Quat. Int. 441, 129–139.
Fick, S.E., Hijmans, R.J., 2017. WorldClim 2: new 1-km spatial resolution climate surfaces for global land areas. Int. J. Climatol. https://doi.org/10.1002/joc.5086.
Fu, G., Charles, S.P., Yu, J., 2009. A critical overview of pan evaporation trends over the last 50 years. Clim. Chang. 97, 193–214.
Fyfe, J.C., Boer, G.J., Flato, G.M., 1999. The Arctic and Antarctic oscillations and their projected changes under global warming. Geophys. Res. Lett. 26, 1601–1604.
Gao, X., Giorgi, F., 2008. Increased aridity in the Mediterranean region under greenhouse gas forcing estimated from high resolution simulations with a regional climate model. Glob. Planet. Chang. 62, 195–209.
Giosan, L., Syvitski, J., Constantinescu, S., Day, J., 2014. Protect the world's deltas. Nature 516, 31–33.
Gray, L.J., Beer, J., Geller, M., Haigh, J.D., Lockwood, M., Matthes, K., Cubasch, U., Fleitmann, D., et al., 2010. Solar influences on climate. Rev. Geophys. 48. https://doi.org/10.1029/2009RG000282.
Greve, P., Orlowsky, B., Mueller, B., Sheffield, J., Reichstein, M., Seneviratne, S.I., 2014. Global assessment of trends in wetting and drying over land. Nat. Geosci. 7, 716–721.
Hansen, J., Sato, M., Kharecha, P., Beerling, D., Berner, R., Masson-Delmotte, V., Pagani, M., Raymo, M., et al., 2008. Target atmospheric CO_2: where should humanity aim? Open Atmos. Sci. J. 2, 217–231.
Huang, J., Sun, S., Zhang, J., 2013. Detection of trends in precipitation during 1960–2008 in Jiangxi province, Southeast China. Theor. Appl. Climatol. 114, 237–251.
Huang, J., Yu, H., Guan, X., Wang, G., Guo, R., 2016. Accelerated dryland expansion under climate change. Nat. Clim. Chang. 6, 166–172.
Ionita, M., 2014. The impact of the East Atlantic/Western Russia pattern on the hydroclimatology of Europe from mid-winter to late spring. Climate 2, 296–309.
Ionita, M., Rimbu, N., Chelcea, S., Patrut, S., 2013. Multidecadal variability of summer temperature over Romania and its relation with Atlantic Multidecadal Oscillation. Theor. Appl. Climatol. 113, 305–315.
IPCC, 2007. Climate change 2007: the physical science basis. In: Solomon, S., et al. (Eds.), Contribution of Working Group I to the Fourth Assessment Report of the Intergovernmental Panel on Climate Change. Cambridge University Press, Cambridge.
IPCC, 2013. Climate change 2013: the physical science basis. In: Stocker, T.F. (Ed.), Contribution of Working Group I to the Fifth Assessment Report of the Intergovernmental Panel on Climate Change. Cambridge University Press, Cambridge.
Irannezhad, M., Marttila, H., Kløve, B., 2014. Long-term variations and trends in precipitation in Finland. Int. J. Climatol. 34, 3139–3153.
Irannezhad, M., Torabi Haghighi, A., Chen, D., Kløve, B., 2015. Variability in dryness and wetness in central Finland and the role of teleconnection patterns. Theor. Appl. Climatol. 122, 471–486.
Jung, M., Reichstein, M., Ciais, P., Seneviratne, S.I., Sheffield, J., Goulden, M.L., Bonan, G., Cescatti, A., et al., 2010. Recent decline in the global land evapotranspiration trend due to limited moisture supply. Nature 467, 951–954.
Kar, G., Verma, H.N., 2005. Climatic water balance, probable rainfall, rice crop water requirements and cold periods in AER 12.0 in India. Agric. Water Manag. 72, 15–32.
Kendall, M.G., 1975. Rank Correlation Methods, fourth ed. Charles Griffin, London.
Knežević, S., Tošić, I., Unkašević, M., Pejanović, G., 2014. The influence of the East Atlantic Oscillation to climate indices based on the daily minimum temperatures in Serbia. Theor. Appl. Climatol. 116, 435–446.
Knight, J.R., Folland, C.K., Scaife, A.A., 2006. Climate impacts of the Atlantic Multidecadal Oscillation. Geophys. Res. Lett. 33. https://doi.org/10.1029/

2006GL026242.
Krichak, S.O., Alpert, P., 2005. Decadal trends in the East Atlantic-West Russia pattern and Mediterranean precipitation. Int. J. Climatol. 25, 183–192.
Krichak, S.O., Kishcha, P., Alpert, P., 2002. Decadal trends of main Eurasian oscillations and the Eastern Mediteranean precipitation. Theor. Appl. Climatol. 72, 209–220.
Lenton, T.M., Held, H., Kriegler, E., Hall, J.W., Lucht, W., Rahmstorf, S., Schellnhuber, H.J., 2008. Tipping elements in the Earth's climate system. PNAS 105, 1786–1793.
Łupikasza, E.B., Hänsel, S., Matschullat, J., 2011. Regional and seasonal variability of extreme precipitation trends in southern Poland and central-eastern Germany 1951–2006. Int. J. Climatol. 31, 2249–2271.
Maeda, E.E., Wiberg, D.A., Pellikka, P.K.E., 2011. Estimating reference evapotranspiration using remote sensing and empirical models in a region with limited ground data availability in Kenya. Appl. Geogr. 31, 251–258.
Mann, H.B., 1945. Non-parametric tests against trend. Econometrica 13, 245–259.
Marin, L., Birsan, M.V., Bojariu, R., Dumitrescu, A., Micu, D.M., Manea, A., 2014. An overview of annual climatic changes in Romania: trends in air temperature, precipitation, sunshine hours, cloud cover, relative humidity and wind speed during the 1961–2013 period. Carpath. J. Earth Environ. Sci. 9, 253–258.
Minea, I., Croitoru, A.E., 2017. Groundwater response to changes in precipitations in north-eastern Romania. Environ. Eng. Manag. J. 16, 643–651.
Moore, G.W.K., Renfrew, I.A., 2012. Cold european winters: interplay between the NAO and the East Atlantic mode. Atmos. Sci. Lett. 13, 1–8.
Nastos, P.T., Politi, N., Kapsomenakis, J., 2013. Spatial and temporal variability of the Aridity Index in Greece. Atmos. Res. 119, 140–152.
Nistor, M.M., Gualtieri, A.F., Cheval, S., Dezsi, S., Botan, V.E., 2016. Climate change effects on crop evapotranspiration in the Carpathian Region from 1961 to 2010. Meteorol. Appl. 23, 462–469.
Niu, J., Chen, J., Sivakumar, B., 2014. Teleconnection analysis of runoff and soil moisture over the Pearl River basin in southern China. Hydrol. Earth Syst. Sci. 18, 1475–1492.
NOAA, 2017a. Teleconnection Data Regarding the NAO, AO, SP, EA, EAWR and MJO Indices. Climate Prediction Center, National Oceanic and Atmospheric Administration. http://www.cpc.ncep.noaa.gov/ (accessed 10 September 2017).
NOAA, 2017b. Teleconnection Data Regarding the QBO Index. Physical Division Science, National Oceanic and Atmospheric Administration. https://www.esrl.noaa.gov/psd/data/correlation/qbo.data (accessed 12 September 2017).
NRCA, 2017. Teleconnection Data Regarding the Solar Flux Index. National Research Council of Canada. http://www.spaceweather.ca/solarflux/sx-4-eng.php (accessed 12 September 2017).
Palizdan, N., Falamarzi, Y., Huang, Y.F., Lee, T.S., 2017. Precipitation trend analysis using discrete wavelet transform at the Langat River Basin, Selangor, Malaysia. Stoch. Env. Res. Risk A. 31, 853–877.
Paltineanu, C., Mihailescu, I.F., Seceleanu, I., Dragota, C., Vasenciuc, F., 2007. Using aridity indices to describe some climate and soil features in Eastern Europe: a Romanian case study. Theor. Appl. Climatol. 90, 263–274.
Paltineanu, C., Mihailescu, I.F., Prefac, Z., Dragota, C., Vasenciuc, F., Claudia, N., 2009. Combining the standardised precipitation index and climatic water deficit in characterizing droughts: a case study in Romania. Theor. Appl. Climatol. 97, 219–233.
Patriche, C.V., 2009. Statistical Methods Applied in Climatology. Terra Nostra Publishing House, Iasi, Romania (in Romanian).
Popescu, V.D., Rozylowicz, L., Cogalniceanu, D., Niculae, I.M., Cucu, A.L., 2013. Moving into protected areas? Setting conservation priorities for Romanian reptiles and amphibians at risk from climate change. PLoS ONE 8, e79330. https://doi.org/10.1371/journal.pone.0079330.
Posea, G., Badea, L., 1984. Romania – Landforms (Geomorphological Regions) (in Romanian). Map, Scale 1:750.000. Scientific and Encyclopaedic Publishing House, Bucharest, Romania.
Prăvălie, R., 2016. Drylands extent and environmental issues. A global approach. Earth Sci. Rev. 161, 259–278.
Prăvălie, R., Bandoc, G., 2015. Aridity variability in the last five decades in the Dobrogea region, Romania. Arid Land Res. Manag. 29, 265–287.
Prăvălie, R., Sîrodoev, I., Patriche, C.V., Bandoc, G., Peptenatu, D., 2014a. The analysis of the relationship between climatic water deficit and corn agricultural productivity in the Dobrogea plateau. Carpath. J. Earth Environ. Sci. 9, 201–214.
Prăvălie, R., Sîrodoev, I., Peptenatu, D., 2014b. Detecting climate change effects on forest ecosystems in Southwestern Romania using Landsat TM NDVI data. J. Geogr. Sci. 24, 815–832.
Prăvălie, R., Bandoc, G., Patriche, C., Tomescu, M., 2016a. Spatio-temporal trends of mean air temperature during 1961–2009 and impacts on crop (maize) yields in the most important agricultural region of Romania. Stoch. Env. Res. Risk A. https://doi.org/10.1007/s00477-016-1278-7.
Prăvălie, R., Patriche, C.V., Sîrodoev, I., Bandoc, G., Dumitraşcu, M., Peptenatu, D., 2016b. Water deficit and corn productivity during the post-socialist period. Case study: southern Oltenia drylands, Romania. Arid Land Res. Manag. 30, 239–257.
Prăvălie, R., Zaharia, L., Bandoc, G., Petrişor, A., Ionuş, O., Mitof, I., 2016c. Hydroclimatic dynamics in southwestern Romania drylands over the past 50 years. J. Earth Syst. Sci. 125, 1255–1271.
Prăvălie, R., Patriche, C., Bandoc, G., 2017a. Quantification of land degradation sensitivity areas in Southern and Central Southeastern Europe. New results based on improving DISMED methodology with new climate data. Catena 158, 309–320.
Prăvălie, R., Săvulescu, I., Patriche, C., Dumitraşcu, M., Bandoc, G., 2017b. Spatial assessment of land degradation sensitive areas in southwestern Romania using modified MEDALUS method. Catena 153, 114–130.
PRDD, 2014. Periodic Report Danube Delta – Statement of Outstanding Universal Value of Danube Delta. World Heritage Centre, UNESCO.
Raes, D., 2012. The ET_o Calculator Reference Manual. Food and Agriculture Organization of the United Nations, Land and Water Division, Rome, Italy.
Rimbu, N., Stefan, S., Busuioc, A., Georgescu, F., 2016. Links between blocking circulation and precipitation extremes over Romania in summer. Int. J. Climatol. 36, 369–376.
Roderick, M.L., Rotstayn, L.D., Farquhar, G.D., Hobbins, M.T., 2007. On the attribution of changing pan evaporation. J. Geophys. Res. 34. https://doi.org/10.1029/2007GL031166.
Rodriguez-Puebla, C., Encinas, A.H., Nieto, S., Garmendia, J., 1998. Spatial and temporal patterns of annual precipitation variability over the Iberian Peninsula. Int. J. Climatol. 18, 299–316.
Royston, P., 1982. An extension of Shapiro and Wilk's W test for normality to large samples. Appl. Stat. 31, 115–124.
Rusu, M., Simion, G., 2015. Farm structure adjustments under the irrigation systems rehabilitation in the Southern Plain of Romania: a first step towards sustainable development. Carpath. J. Earth Environ. Sci. 10, 91–100.
Salmaso, N., 2012. Influence of atmospheric modes of variability on a deep lake south of the Alps. Clim. Res. 51, 125–133.
Salmi, T., Maatta, A., Anttila, P., Ruoho-Airola, T., Amnell, T., 2002. Detecting Trends of Annual Values of Atmospheric Pollutants by the Mann–Kendall Test and Sen's Slope Estimates – The Excel Template Application Makesens. Finnish Meteorological Institute, Helsinki, Finland.
Sandu, I., Pescaru, V.I., Poiana, I., Geicu, A., Candea, I., Tastea, D., 2008. The Climate of Romania. Romanian Academy Publishing, Bucharest, Romania (in Romanian).
Scaife, A.A., Arribas, A., Blockley, E., Brookshaw, A., Clark, R.T., Dunstone, N., Eade, R., Fereday, D., et al., 2014. Skillful long-range prediction of European and North American winters. Geophys. Res. Lett. 41, 2514–2519.
Seager, R., Ting, M., Held, I., Kushnir, Y., Lu, J., Vecchi, G., Huang, H.P., Harnik, N., et al., 2007. Model projections of an imminent transition to a more arid climate in Southwestern North America. Science 316, 1181–1184.
Sen, P.K., 1968. Estimates of the regression coefficient based on Kendall's Tau. J. Am. Stat. Assoc. 63, 1379–1389.
Sfîcă, L., Niță, A., Iordache, I., Ilie, N., 2015. Specific weather conditions on Romanian territory for Hess-Berezowsky westerly circulation types. In: Energy and Clean Technologies. Book Series: International Multidisciplinary Scientific Geoconference (SGEM), 15th International Multidisciplinary Scientific Geocongerece (SGEM)pp. 1073–1080 (Albena, Bulgaria).
Sfîcă, L., Iordache, I., Voiculescu, M., 2017. Solar signal on regional scale: a study of possible solar impact upon Romania's climate. J. Atmos. Sol. Terr. Phys. https://doi.org/10.1016/j.jastp.2017.09.015.
Sheffield, J., Wood, E.F., Roderick, M.L., 2012. Little change in global drought over the past 60 years. Nature 491, 435–438.
Spinoni, J., Szalai, S., Szentimrey, T., Lakatos, M., Bihari, Z., Nagy, A., Németh, Á., Kovács, T., et al., 2014. Climate of the Carpathian Region in the period 1961–2010: climatologies and trends of 10 variables. Int. J. Climatol. https://doi.org/10.1002/joc.4059.
Sutton, R.T., Hodson, D.L.R., 2005. Atlantic Ocean forcing of North American and European summer climate. Science 309, 115–118.
Tabari, H., Aeini, A., Hosseinzadeh Talaee, P., Shifteh Some'e, B., 2012. Spatial distribution and temporal variation of reference evapotranspiration in arid and semi-arid regions of Iran. Hydrol. Process. 26, 500–512.
Thompson, D.W.J., Baldwin, M.P., Wallace, J.M., 2002. Stratospheric connection to northern hemisphere wintertime weather: implication for prediction. J. Clim. 15, 1421–1428.
Vicente-Serrano, S.M., Azorin-Molina, C., Sanchez-Lorenzo, A., Revuelto, J., López-Moreno, J.I., González-Hidalgo, J.C., Moran-Tejeda, E., Espejo, F., 2014. Reference evapotranspiration variability and trends in Spain, 1961–2011. Glob. Planet. Chang. 121, 26–40.
Vincente-Serrano, S.M., Beguería, S., López-Moreno, J.I., 2010. A multiscalar drought index sensitive to global warming: the standardized precipitation evapotranspiration index. J. Clim. 23, 1696–1718.
Wang, K., Dickinson, R.E., Wild, M., Liang, S., 2010. Evidence for decadal variation in global terrestrial evapotranspiration between 1982 and 2002: 2. Results. J. Geophys. Res. 115. https://doi.org/10.1029/2010JD013847.
Wilks, D., 2011. Statistical Methods in Atmospheric Science. Academic Press, Massachusetts, United States.
Wong, G.J., Osterberg, E.C., Hawley, R.L., Courville, Z.R., Ferris, D.G., Howley, J.A., 2015. Coast-to-interior gradient in recent northwest Greenland precipitation trends (1952–2012). Environ. Res. Lett. https://doi.org/10.1088/1748-9326/10/11/114008.
XLSTAT, 2017. Data Analysis and Statistical Solution for Microsoft Excel. Addinsoft, Paris, France.
Yeo, S.R., Kim, W.M., Kim, K.Y., 2017. Eurasian snow cover variability in relation to warming trend and Arctic oscillation. Clim. Dyn. 48, 499–511.
Zampieri, M., Toreti, A., Schindler, A., Scoccimarro, E., Gualdi, S., 2017. Atlantic multi-decadal oscillation influence on weather regimes over Europe and the Mediterranean in spring and summer. Glob. Planet. Chang. 151, 92–100.
Zhang, K., Kimball, J.S., Mu, Q., Jones, L.A., Goetz, S.J., Running, S.W., 2009. Satellite based analysis of northern ET trends and associated changes in the regional water balance from 1983 to 2005. J. Hydrol. 379, 92–110.
Zhao, G., Li, E., Mu, X., Wen, Z., Rayburg, S., Tian, P., 2015. Changing trends and regime shift of streamflow in the Yellow River basin. Stoch. Env. Res. Risk A. 29, 1331–1343.